DETERMINATION OF GEOMETRIC UNCERTAINTIES AND THEIR INCLUSION INTO MARGINS FOR THREE DIMENSIONAL CONFORMAL RADIOTHERAPY OF THE PROSTATE

NIKKI CASWELL
SCHOOL OF CHEMISTRY AND PHYSICS
THE UNIVERSITY OF ADELAIDE
NOVEMBER 2005

THIS DISSERTATION IS SUBMITTED AS PARTIAL FULFILMENT OF THE DEGREE MASTER OF SCIENCE (MEDICAL PHYSICS)

TABLE OF CONTENTS

TABLE OF FIGURES

TABLE OF TABLES

1 Abstract

With the advent of three dimensional conformal radiotherapy (3D CRT) techniques, and more recently intensity modulated radiotherapy (IMRT), there has been a general trend to reduce the dose to normal tissues treated. This can be achieved by reducing the margin applied to the clinical target volume (CTV) to form the planning target volume (PTV). As the size of this margin has approached the magnitude of the geometric uncertainties involved in 3D CRT, determining these uncertainties for individual centres and treatment techniques has become increasingly necessary.

A determination of set-up, organ motion and target delineation uncertainty was undertaken. Random and systematic set-up uncertainty was determined by an electronic portal imaging (EPI) study. EPI images for 62 patients, with an average of 10 images per patient, were analysed by matching bony anatomy on EPI images to the same anatomy on reference digitally reconstructed radiographs (DRRs). The random set-up uncertainty (1 standard deviation), after the application of a patient correction protocol, was 2.4mm left/right (LR), 2.06mm anterior/posterior (AP), 2.0mm superior/inferior (SI) and the systematic component was 1.57mm LR, 1.37mm AP 1.02mm SI.

Inter-fraction organ motion for the prostate and the rectum were estimated by the movement of the centroid of each structure outlined on sequential CT scans. Several methods for calculating centroid co-ordinates from structure outlines were investigated. It was resolved that the centroid as determined by the planning system was insufficiently accurate for use in detecting the size of movements expected. An Excel macro was developed and used to calculate the centroids that were subsequently used to determine both organ motion and intra-observer target delineation.

Organ motion uncertainty (1 standard deviation), of the prostate was 1.2mm LR, 3.1mm AP, 4.6mm SI and 1.4mm LR, 3.5mm AP, 8.3mm SI for the rectum. Prostate motion was found to correlate with the fractional change in rectal volume.

To determine intra-observer variability the prostate and rectum were outlined 3 times, for 6 patients on 12 CT scans by a single observer. The position of the centroid for each outline was used to quantitate the intra-observer target delineation uncertainty (root mean square of the individual standard deviations); which was 0.37mm LR, 1.10mm AP, 1.45mm SI for the prostate and 0.43mm LR, 1.30mm AP, 2.66mm SI for the rectum.

These uncertainties were combined to calculate a CTV-PTV margin. The CTV-PTV margin was calculated using two methods; one based on physical constraints (McKenzie et al, 2000) and one based on biological constraints (van Herk et al, 2000). The CTV-PTV margin calculated by using the McKenzie et al (2000) method yielded a margin of 2.7mm LR, 7.6mm AP, 12.6mm SI. The van Herk et al (2000) margin calculation resulted in a CTV-PTV margin of 3.7mm LR, 8.1mm AP, 12.3mm SI.

The values for the uncertainties determined in the study were consistent with previously published studies. This study showed the ability of an offline set-up correction protocol to reduce systematic set-up errors, and highlighted the larger uncertainties of organ motion and target delineation. These uncertainties have been shown to be non-trivial and must be considered when a decision is made to reduce margins. A CTV-PTV margin was calculated which will account for these uncertainties.

Statement Regarding Originality, Loan and Photocopying of Thesis

This work contains no material which has been accepted for the award of any other degree or diploma in any university or other tertiary institution and, to the best of my knowledge and belief, contains no material previously published or written by another person, except where due reference has been made in the text.

I give consent to this copy of my thesis, when deposited in the University Library, being available for loan and photocopying, subject to the provisions of the Copyright Act 1968.

23/01/2008

Nikki Caswell Date

Acknowledgements

I'd like to thank lots of people; but it isn't possible to mention everyone individually. Following are some who deserve a specific mention.

I'd like to thank my supervisors, Annette Haworth, Tim van Doorn and Martin Ebert, for their advice and patience throughout the project. To Annette for introducing me to the world of the prostate and passing the sickness on to me. I owe Martin a debt of gratitude for helping me keep on track, reassuring me and most of all knowing when to push and more importantly when not to push during the hard times. Martin was also kind enough to write and process the IDL centroid calculations. Thanks to Jane, Adehlia and Roseanna Ebert who have made me welcome in their home when I have come to meet Martin.

David Waterhouse, who spontaneously provided me with the Excel macro to determine centroids from RTOG data, is a star. Thanks to Graham Rickman for teaching me how to plan 3D CRT treatments, teaching me some of the many nuances of the CMS planning system, and entertaining me with the many adventures of his new puppy dog. To Dr Mandy Taylor, for "ring around a prostate" and "ring around a rectum", the chocolates were not thanks enough for the time you put in.

Thanks to Dr Rodney Pinna for the novel application of offshore structural engineering techniques to the wonderful world of prostates and rectums, for inputting the RTOG data into Patran and producing the finite element volumes. To Rod's colleague who shared his office, my apologies for making you feel uncomfortable to the point of leaving after my excited ramblings about "my prostates and my rectums". To all the staff at the Department of Radiation Oncology at Sir Charles Gairdner Hospital who all in some way or another made this project possible. To the Mighty Reds, LFC for winning the European Cup for the 5th time on that one night in May.

To Mr Boots and Raji who provided the kind of support a cat and dog only can.

Most importantly to Heath, for providing support, comfort, skills with formatting and many a meal. For being a sounding board and letting me yell and scream about my frustrations and letting me cry during the bad times that happened to coincide with this project. For making the biggest sacrifice in allowing me to go half way around the world to be able to escape all other commitments and concentrate on getting this finished.

2 Introduction

2.1 The External Beam Radiotherapy Process

Radiotherapy involves the precise and accurate application of radiation (typically megavoltage X-rays or electrons) to tissues with the aim of killing tumour cells and sparing normal tissues. Radiation dose needs to be applied in such a way to ensure tumour coverage whilst minimising dose to normal tissues. Normal tissue dose can result in unwanted side effects.

Movement of the tumour volume relative to the radiation beam can reduce dose coverage. To account for uncertainty in prostate position and to ensure the CTV receives the prescribed dose, margins must be defined around the CTV. Quantification of these uncertainties and their incorporation into treatment planning will aid in delineating an appropriate PTV.

Conformal radiotherapy techniques offer the potential to decrease target margins and hence decrease the dose to normal tissues. The increasing conformity of external beam radiotherapy treatments (EBRT) coupled with the desire to increase tumour doses in search of increased local control has highlighted the need to quantify, minimise and incorporate into planning the geometric uncertainties associated with these treatments (Booth et al, 1999).

The margins added to the CTV, designed to account for these uncertainties in order to avoid not only a geographical miss but to limit unwanted dose to any organs at risk (OR), are defined in the International Commission of Radiation Units (ICRU) Report Numbers 50 and 62 (see Appendix 7.3 for definitions).

Once the clinical decision is made for treatment with EBRT a chain of events that lead to the eventual application of external beam radiation begins. These can be broadly separated into two sections, treatment preparation and treatment execution (van Herk, 2004). Table 1 shows the steps and events involved in the process.

Treatment Preparation	Imaging
	Patient mark up
	Structure Definition
	Beam modelling
	Dose calculation
	Export of data to record and verify system
	Simulation/verification
Treatment Execution	Patient set-up
	Portal imaging
	Delivery of beams

Table 1: General process of external beam radiotherapy

2.2 Geometric Uncertainties Encountered in CT Planned External Beam Radiotherapy

Geometric uncertainties can enter at any point in the chain of events that occur from the acquisition of the treatment planning image through to delivery of each individual fraction in a course of EBRT. Geometric uncertainties can be systematic or random in nature. In this document the term uncertainty and error are assumed to be the same and can be used interchangeably.

At the CT scanner a number of uncertainties are introduced which are of a systematic nature. That is for a given patient the uncertainty induced will propagate through the entire treatment process. Some sources of these uncertainties can be misalignment of the CT room lasers, error between the CT couch readout and its true position, error in the longitudinal motion of the CT couch, distortion of the CT image and errors introduced when transferring digital images between image-processing/handling systems. Regular quality assurance procedures to evaluate and minimise the differences between the CT and treatment machine are an integral component of a radiotherapy department's quality assurance protocol. Summaries of commissioning and ongoing quality tests to quantify geometric errors between CT and treatment can be found in Mutic et al (2003). Systematic errors introduced at CT are incorporated into the total systematic set-up error described in Section 3.1.

Organ motion is also introduced at the time of the treatment planning computerised tomography (TPCT) scan as the TPCT scan takes a snapshot of the moving organ in space and beams are placed according to the position of organs at that time. Organ motion during a TPCT scan (i.e., respiratory, cardiac, gastrointestinal and general patient motion), introduces further uncertainties in certain anatomical sites as well as artefacts and blurring in the TPCT.

At the radiotherapy treatment planning system (RTPS) the target and critical structures are delineated, to which there is an associated error. There may be errors introduced when importing the TPCT scan into the RTPS, in the form of minor differences in orientation of the scan. If the automatic RTPS function to grow a

PTV from a CTV (see Appendix 7.3 for definitions) is used then the algorithm that it uses to achieve this may introduce a further error. There may be discrepancies between the model of the beam in the RTPS and measured data for that same beam.

At the linear accelerator there are a number of factors and processes that can introduce geometric errors, for example, misaligned lasers, isocentre position, and multi-leaf collimator leaf position. Set-up error, both systematic and random, can occur at the linear accelerator. Systematic set-up error may result from differences between the CT and linear accelerator couches or differences in set-up, for example the positioning of limbs can have an effect on the position of internal organs. Random set-up errors can be caused by the patient themselves, the experience of the radiation therapist in setting up patients and the time available to the radiation therapist to set the patient up (Hurkmans et al, 2001). Another important area of uncertainty is organ motion, that is the internal movement of the organ relative to bony anatomy and skin marks with respect to its position on the TPCT scan. In this instance the organ motion uncertainty is a random error, as apposed to a systematic error as is the case at the time of the TPCT scan. Anatomical changes can occur within a patient between the TPCT and treatment and between treatments (e.g., weight loss/gain, amount of bowel gas, bladder filling) which can lead to organ motion and deformation.

2.3 Hypotheses and Aims

The purpose of this project was to determine that errors associated with set-up, organ motion and target delineation in three dimensional conformal radiotherapy of the prostate at the Department of Radiation Oncology at Sir Charles Gairdner Hospital (SCGH), Western Australia were of a similar magnitude to those reported in the literature. These uncertainties can be population, technique, institution and in the case of target delineation doctor dependent. The aims associated with this hypothesis were to:

- Quantify daily prostate patient set-up errors based on bony anatomy via portal imaging.
- Estimate typical ranges of organ motion (PTV and rectum) for prostate patients via two separate CT imaging studies.
- Quantify voluming errors introduced by intra-observer variation.

As part of this investigation the question of the accuracy of centroid definition by a commercial RTPS could misrepresent the errors determined using this quantity was raised. To address this, an evaluation of the RTPS and alternative methods for determining centroid was carried out.

Furthermore, assessment of the incorporation of these uncertainties into margins for conformal EBRT of the prostate was carried out to show that reductions of margins must be considered in relation to the errors in individual clinics for individual techniques. To address this the following was undertaken:

- Calculate a CTV-PTV margin from the set-up, intra-observer delineation and organ motion uncertainties.

The relative magnitude of patient set-up, organ motion and delineation errors were examined in relation to margin sizes.

2.4 Set-up, Organ Motion and Target Delineation Errors

Uncertainties associated with daily set-up, organ motion and target delineation have been the subject of many studies by various institutions (Hamilton et al, 2005). Errors associated with EBRT treatments are generally defined in the three principle axes relative to the patient, left-right (LR), anterior-posterior (AP) and superior-inferior (SI).

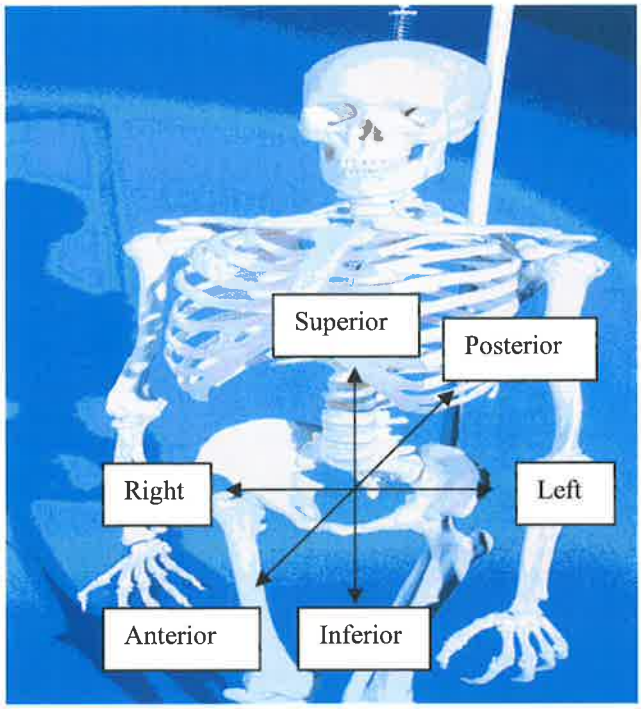

Figure 1: Three principle patient axes

Set-up error quantifies the potential differences between the positioning of the patient at the time of CT relative to the time of treatment. Set up error has both systematic and random components. Components of set-up error can be assessed by means of portal imaging. A reference image, simulator film or digitally reconstructed radiograph, is taken. The reference image shows the treatment field edge, anatomical landmarks and if used implanted fiducial markers (Hurkmans et al, 2001). These are used to match the treatment portal images to the reference image. The mismatch between the treatment portal image and the reference image is the combined set-up error. This error will include both the random and systematic components, which cannot be separated by a single matched pair of images

(Greener, 2003). The acquisition of multiple images will allow for the separation of these components, the number of images acquired and the number of patients imaged will influence the accuracy of the determined components (Greener, 2003). To accurately determine the systematic and random components of set-up error it has been suggested that data sets for 20 or more patients with treatment images obtained weekly are required (Greener, 2003). The standard deviation of the random set-up error ($\sigma_{set\text{-}up}$) and the standard deviation of the systematic set-up error ($\Sigma_{set\text{-}up}$) is a common method of reporting set-up accuracy.

Set-up errors as determined using portal imaging and matching to bony anatomy have been reported by many authors, Table 2 contains a brief summary of some of these. The errors reported vary, however are generally of the order of millimetres. This variation in set-up error indicates a requirement for centres to carry out their own analysis of set-up accuracy rather than relying on values taken from the literature.

		Systematic Error 1SD (mm)			**Random Error 1SD (mm)**		
Study	**Number of image pairs**	**LR**	**AP**	**SI**	**LR**	**AP**	**SI**
Bijhold et al (1992)	105	1.2	1.2	2.3	1.8	1.9	2.1
el-Gayed et al (1993)	260	2.2	1.4	1.0	1.7	1.9	1.2
Bel et al (1996)	2415	2.3	2.7	2.2	2.1	2.0	2.0
Greer et al (1998)	159	-	3.7	-	-	2.3	-
	205	-	1.2	-	-	1.3	-

Table 2: Summary of set-up errors reported by various authors determined using portal imaging (electronic or film)

Implanted markers have also been used to assess set-up errors. Litzenberg et al (2002) analysed set-up in prone and supine positions using markers implanted in the prostate. The set-up errors for the supine were shown to be lower than those for the prone (Litzenberg et al, 2002). Chung et al (2004) determined set-up error using 3 implanted gold markers. Set-up error of the centre of mass of the implanted markers prior to any correction was 3.2mm AP and 2.5mm SI (Chung et al, 2004).

Ultrasound is becoming a popular way to image the prostate for treatment localisation. D'Souza et al (2003) used ultrasound localisation for 20 patients with an average of 26 ultrasound localisations. Their results show a $\Sigma_{set\text{-}up}$ of 1.4mm LR, 3.6mm AP and 3.5mm SI and a $\sigma_{set\text{-}up}$ of 2.9mm LR, 2.6mm AP and 3.4mm SI (D'Souza et al, 2003). A study combining daily ultrasound localisation and weekly portal imaging showed a set-up error of 2.8mm LR, 3.0mm AP and 2.0mm SI using ultrasound and 3.2mm LR, 6.4mm AP, 6.4mm SI using portal imaging (Little et al, 2003).

Organ motion can be separated into two types; inter-fraction and intra-fraction motion. Inter-fraction motion is the motion that occurs between the TPCT scan and subsequent treatment fractions; this has both systematic and random components. Intra-fraction motion refers to the motion that occurs during a treatment fraction.

Studies reviewing inter-fraction motion have been carried out using serial imaging with and without implanted fiducial markers. Balter et al (1995) investigated the movement of the prostate by use of implanted radiopaque markers and portal imaging. This study found that typical motion of the prostate is small, but its motion is significantly larger in the AP and SI directions than in the LR direction (Balter et al, 1995). Patients previously implanted with I-125 seeds for treatment have been retrospectively repeatedly simulated to assess prostate motion (Althof et al, 1996). Althof et al (1996) reported standard deviations (1 SD) of 0.8mm LR, 1.5mm AP and 1.7mm SI. Rudat et al (1996) assessed motion of the prostate using a single isocentric CT slice, motion in the SI direction could not be determined. Prostate movement in the AP direction was determined to be significantly larger

than LR, the standard deviations (1 SD) of the prostate motion were 3.7mm and 1.9mm (Rudat et al, 1996).

van Herk et al (1995) took 3 CT scans and co-registered them to the original TPCT. Motion of the prostate, represented as 1 standard deviation, relative to the pelvic bone was 0.9mm LR, 2.7mm AP and 1.7mm SI (van Herk et al, 1995). Rectal filling was shown to influence both the rotation of the prostate in the LR axis and translation in the AP direction (van Herk et al, 1995). A study by Stroom et al (1999) investigated prostate motion in both the supine and prone treatment positions. Their results were 0.6mm LR, 2.8mm AP and 2.8mm SI (1 SD) supine and 0.5mm LR, 2.1mm AP and 1.7mm SI (1 SD) prone (Stroom et al, 1999). Roeske et al (1995) used weekly CT to assess prostate motion in 10 patients. AP prostate motion correlated with the change in rectal volume (Roeske et al, 1995). Tinger et al (1998) also reported a correlation of AP prostate motion with the fractional change in rectal volume.

Target delineation error is a systematic error as once the structure has been outlined it will be the same for each treatment fraction, and its effect will be propagated down the treatment chain (McKenzie et al, 2003). This error can arise from the limitations in resolution of imaging modalities to define the structure. This is particularly the case in the direction perpendicular to the image slice planes. The resolution in that direction, usually cranio-caudally, is dependent on the slice thickness and slice separation and is prone to the partial volume effect. The partial volume effect arises due to the finite size of the voxels and the possibility of a structure varying rapidly over a similar distance. Hence, it is quite often observed that the delineation error is greater in this direction.

Target delineation error can be introduced via inter-modality variation. That is the same target drawn on different imaging modalities (eg CT and MRI) can be significantly different (Graham et al, 2003). There is also both inter-observer and intra-observer errors. Inter-observer target delineation error is determined by having a number of observers outline the same target and calculating the variation in their outlined structures. Intra-observer target delineation error involves a single

observer outlining the same target on a number of occasions separated in time, and determining the variation.

There have been a number of studies attempting to quantify target delineation error for the pelvic region (Livsey et al, 2004, Logue et al 1998, Fiorino et al, 1998, Seddon et al, 2000). Most of these papers examine inter-observer variability, which was found to be significant. For the purposes of this project one observer and one imaging modality was used to determine the intra-observer target delineation error, which shall be denoted as $\Sigma_{delineation}$. This will be inclusive of the error introduced due to the limitations of the imaging modality used as described above.

2.5 Carcinoma of the Prostate

The prostate is a pear shaped glandular organ of the male reproductive system. The size of a normal prostate is similar to that of a chestnut or walnut (Marieb et al, 2001). The prostate's function is to produce secretions that contribute to seminal fluid (Marieb et al, 2001). Anatomically the prostate is located inferior to the bladder, anterior to the rectum and surrounds urethra (Dobbs J et al, 1999).

Cancer is characterised by the uncontrolled growth of abnormal cells (Leaver et al, 2004). In the prostate it is generally considered a relatively slow growing cancer; however the tumours can put pressure on the urethra making it difficult and painful to urinate (Tortora et al, 1993). The cancer can extend beyond the capsule of the prostate and can, in advanced stages, lead to distant metastases.

According to the Australian Bureau of Statistics (ABS) prostate cancer is the second most common cause of cancer death amongst males in Australia. According to the 1999 ABS data, prostate cancer is responsible for 13% of all male cancer deaths. Prostate cancer incidence rates increased with the introduction of prostate specific antigen (PSA) testing (Smith et al, 1998). The five-year survival rate for prostate cancer for the period 1992-1997 was 82.7% (Australian Bureau of Statistics, 2005). The high probability of long term survival coupled with an increased incidence in an ageing population has led to considerable research into the treatment of this disease.

The range of treatment options available is dependent on the stage of the disease. The options available to patients generally are watchful waiting, androgen deprivation hormonal therapy (ADHT), radical prostatectomy, EBRT and brachytherapy. Treatment regimes often include combination of therapies. Watchful waiting, ADHT, radical prostatectomy and prostate seed implant brachytherapy alone are considered options for low risk patient's whose disease has not breached the prostatic capsule (Dobbs et al, 1999). For intermediate to high risk patients', whose disease has breached the prostatic capsule, combinations of ADHT, EBRT and high dose rate brachytherapy are often employed. Conventional EBRT

and radical prostatectomy have similar survival rates for these patients (Dobbs et al, 1999).

Increases in dose delivered by EBRT have been shown to increase freedom from local failure (Zelefsky et al, 1998). In order to be able to increase the prescription dose without increasing dose to normal tissues, treatment plans have become increasingly conformed to the PTV with three dimensional conformal radiotherapy (3D CRT) and intensity modulated radiotherapy (IMRT). With these techniques margins have become tighter and dose gradients at the edge of the PTV have become steeper. As a consequence geometric uncertainties have become increasingly important to quantify and if possible reduce. Portal imaging to assess and reduce set-up uncertainties has become common practice when treating with 3D CRT and IMRT (Bel et al, 1996). Methods such as implanted radiopaque markers, ultrasonography and cone beam CT are being increasingly used to attempt to localise the prostate as apposed to bony anatomy.

2.6 The Process of External Beam Prostate Conformal Radiotherapy at Sir Charles Gairdner Hospital

Once the decision has been made for EBRT to be delivered the patient undergoes a TPCT scan. The CT takes place on a GE Medical Systems LxI (GE Medical Systems, Fairfield CT) single slice CT scanner. The CT couch has a flat insert to mimic the couch on the linear accelerator. The patient is set up supine with a support under the knees and at the ankles. The support devices aid in patient positioning. At the time of this scan the patient will be aligned using the lasers in the CT room. The lasers are the same as those fitted in the linear accelerator bunkers, with the assumption the CT room co-ordinates are the same as that of each linear accelerator bunker. The patient's skin is marked with tattoos and fiducial markers. The tattoos and fiducial markers are placed at midline on the anterior surface and at mid–separation laterally. The CT scan is taken with a 3mm slice thickness, 3mm slice spacing and the zero slice going though the fiducials. The CT slices are contiguous from the top of the pelvic brim to just below the ischial tuberosity.

The scan is then transferred to the RTPS XiO, (Computerized Medical Systems, St Louis, MO). A study set containing the CT scan is created, and an automatic external contour is created in the Patient File Maintenance module. A CT number to electron density conversion for the GE LxI CT scanner is applied to the CT data set.

The study set is transferred to FocalSim (Computerized Medical Systems, St Louis, MO) where the Radiation Oncologist will outline the target volume. The Gross Tumour Volume (GTV) will be outlined, which is equivalent to the CTV. The Radiation Oncologist will then request margins to be added to this structure to form PTV1, the phase 1 volume, and PTV2, the phase 2 volume. The Radiation Therapist will mark on the organs at risk including the femurs and the rectum. The femurs are outlined from the top of the femoral head to the level of the lesser trochanter. The rectum is defined from the sacro-illiac junction to 1.5cm (5 CT slices) beyond the prostatic apex.

The study set which now includes the contours is transferred back to the XiO RTPS. The planning is carried out using template plans in XiO. The phase 1 template plan has its isocentre placement at the centre of PTV1. The phase 1 template plan has 5 primary beams, Posterior 180°, Right Lateral Oblique 260°, Right Anterior Oblique 324°, Left Anterior Oblique 36° and Left Lateral Oblique 100°. There are six other beams which are segments of the primary beams. These segmented beams are used to boost the dose to PTV1 whilst shielding organs at risk in particular the rectum. Multi leaf collimation is used to provide field shaping and rectal shielding. The field length is decided by the Radiation Oncologist based on the number of slices included in the PTV1; this is the 95% field length. The 50% field length is determined by taking the average source to skin distance and using this along with the 95% field length in a look up table. This length is then used for all fields. Phase 1 of treatment for this study group consisted of 5 weeks (25 fractions, 2Gy per fraction) of treatments followed by 2 weeks (10 fractions, 2Gy per fraction) of a phase 2 treatment.

The template plan for phase 2 has the same isocentre as phase 1. In phase 2 only the primary beams are treated and the field length is adjusted to PTV2. The plan is designed to achieve 95% of the prescription dose to the PTV for each phase.

The dose is calculated with a 0.25cm dose calculation grid. Anterior and lateral Digitally Reconstructed Radiographs (DRRs) are created and along with the planning details are electronically transferred to the record and verify system for the linear accelerator.

At every treatment fraction the patient is set-up using the treatment room lasers to the external skin tattoos, making any shifts to isocentre from these marks. EPIs were generally acquired daily in the first week of treatment and then weekly thereafter, to be compared to the DRR produced by the RTPS. Anatomical landmarks and the field edge can be seen on both the DRRs and the portal image. These details are used to perform the match between the DRR which represents the patient's planned position and the portal image which represents the patient's

treatment position. This is to verify isocentre and any shifts required to place the patient in the planned position are performed prior to the subsequent fraction.

3 Methods and Materials

3.1 Set-up accuracy study

Patients were set-up supine with a knee support and ankle support in the same position as their TPCT scan. Set-up accuracy was determined by way of daily EPI, manually matched to the bony anatomy on the DRR from the RTPS. Orthogonal, left lateral and posterior, DRRs were created in the XiO RTPS. These were exported to PortalVision (Varian Medical Systems, Palo Alto, CA).

Left lateral and posterior EPI images were captured on the treatment machine using PortalVision software. Within PortalVision, the DRR and EPI are overlayed and the EPI image is translated until the bony anatomy matches that on the DRR. This procedure is carried out for the left lateral and posterior DRR/EPI pairs. AP and SI shifts are obtained from the left lateral DRR/EPI pair; LR and SI shifts are obtained from the posterior DRR/EPI pair. The matching was completed by a Senior Radiation Therapist with experience in image matching to reduce the introduction of errors from inter-observer variation. Intra- and inter-observer variability in image matching was not measured as part of this study. Deviations were recorded and analysed in Excel (Microsoft, Redmond, WA).

This process was originally carried out for a small pilot group of patients (P=10), treated over a period of weeks, with an average of 29 images per patient. The same analysis was performed for a larger group of patients (P=62), treated over a period of some months, with an average of 10 images per patient.

Variations in patient position were examined by repeated portal imaging. Identified systematic set-up errors were corrected with the result that the percentage of set-up errors within 5 mm of planned isocentres was greater than 90%. The patient position correction protocol in place at the time this group of patients was treated did not necessarily follow any of the well-known published methods like the Newcastle Method (Denham et al, 1993) or the NKI method (Bel et al 1993). The patient position correction protocol used electronic portal images; acquired during the first 3 fractions of treatment and weekly beyond that. Any deviation of greater

than 5mm in any one direction was corrected at the next fraction. A deviation of 3-5mm would not be corrected at the next fraction but another EPI would be acquired at the next fraction. If this was consistent with the previous fraction the set-up would be corrected, i.e. the patient would be moved. A deviation of less than 3mm was acceptable. Any correction would be followed up with an EPI, to ensure that the move had corrected the deviation to within the acceptable range.

The original data (corrected data) consisted of deviations from isocentre that had been corrected by the patient position correction protocol. Any analysis of this data would only be relevant to patients treated in this manner. However the information about the corrections made was available therefore it was possible to remove the effect of the patient position correction protocol and determine the set-up errors for the patients assuming the patient position correction protocol was not applied (uncorrected data). These data, consisting of the isocentre positions and any shifts applied, for both the pilot group (n=10) and the study group (n=62) is listed in table 18 and 19.

The determination of the systematic and random errors for both groups of patients was carried out according to the methodology outlined by Greener (2003). By comparing an EPI with its reference DRR the error determined will be a combination of the systematic and random components. Comparing multiple images for multiple patients and using statistical methods these components can be separated (Greener, 2003).

As the method proposed by Greener (2003) is a statistical approach, the accuracy of the errors determined will be dependent on the number of images and the number of patients used in the study. The errors reported are the standard deviation of the random set-up error ($\sigma_{set\text{-}up}$) and the standard deviation of the systematic set-up error ($\Sigma_{set\text{-}up}$). Accurate determination of $\sigma_{set\text{-}up}$ can be done with small numbers of patients however $\Sigma_{set\text{-}up}$ needs larger numbers of patients, greater than 10 (Greener, 2003). Greater than or equal to 20 patients, with a minimum of weekly imaging, are required for an accurate estimate of $\Sigma_{set\text{-}up}$ and $\sigma_{set\text{-}up}$. The equations 5.1 and 5.2 are

those proposed by Greener (2003) and used in the analysis of the data presented in this thesis (shown in Appendix 7) for the determination of $\sigma_{set\text{-}up}$ and $\Sigma_{set\text{-}up}$.

$$\sigma_{set-up} = \sqrt{\frac{1}{N-P}\sum_{p=1,P}\sigma_{inter,p}^{2}\left(n_p - 1\right)} \tag{5.1}$$

$$\Sigma_{set-up} = \sqrt{\frac{P}{N(P-1)}\sum_{p=1,P} n_p\left(m_p - m_{overall}\right)^2} \tag{5.2}$$

Where:

N is the total number of images in the study.

P is the total number of patients for which images were acquired.

$\sigma_{inter,p}$ is the standard deviation of the inter-fractional random treatment set-up error for patient p in a given direction.

n_p is the number of images taken for patient p.

m_p is the mean deviation for given parameter for patient p for all images taken n_p.

$m_{overall}$ is the overall mean population error for the measured parameter.

3.2 Organ motion study

Organ motion was assessed by means of sequential Computerised Tomography (CT) scans. The first was the treatment planning CT scan (TPCT). The second was taken nominally after 5 weeks of treatment, which corresponds with the commencement of the second phase of treatment as described in Section 2.6. Patients were instructed to have their bladder "comfortably full" - no instructions were provided regarding rectal filling. Patients were scanned in the supine position using 3mm slices on a GE LxI CT scanner (GE Medical Systems, Fairfield CT). FocalFusion (Computerized Medical Systems, St Louis, MO) was used to co-register the two CT image sets and a radiation oncologist outlined the prostate and the rectum.

The data were then electronically transferred back via the local area network (LAN) to the RTPS, XiO (Computerized Medical Systems, St Louis, MO), which was used to export the contour information in Radiation Therapy Oncology Group (RTOG) format for determination of the centroid of the structures (see Appendix 7.2 for further information). The displacement of the centroid between the TPCT and the 2^{nd} scan was used as the measure of organ motion for this study.

Internal organ motion is mainly due to the involuntary motion or deformation of other organs that are part of or next to the digestive or respiratory systems. For the example of the prostate, the state of the rectum has been shown to influence the movement of the prostate (Tinger et al, 1998, Roeske et al, 1995). It is logical then to presume that the magnitude and direction of the prostate movement be related to the rectal filling protocols of individual clinics. Motion of the prostate was analysed with respect to fractional change in rectal volume, rectal volume and the motion of the rectum.

3.2.1 Determination of organ centroid

A method of measuring the amount of organ motion between the two CT scans was required. Organ motion was measured by comparing the displacement of the centroid of the organ on the TPCT scan with the centroid on the subsequent CT scan.

The XiO RTPS allows the placement of an interest point at the centre of a contoured organ, and its co-ordinates can be obtained thus allowing a measurement of organ motion. However XiO uses a simplistic method when determining the centroid. XiO forms a bounding box around the maximum extent of the structure then calculates the centre of the box. This algorithm is limited in its accuracy as the calculation does not account for the full spatial extent of the volume. This method might not be sensitive to small movements that were expected for prostate and rectal organ motion. Three additional methods of determining the centroid of an organ were therefore investigated, these methods utilised the contour files exported from XiO using the RTOG Data Submission Export function (Harms WB et al, 1997).

3.2.1.1 Finite element model

The points defining contours are not regularly spaced on each image slice. As such, it is not possible to calculate the geometric centre of points by averaging their X and Y coordinates. More complex methods were required to estimate the true centroid position. MSC Patran (MSC Software) is a 3-D mechanical computer aided-engineering (MAE) software package utilising finite element modelling. Patran was used to read in the data points and form closed loops in the two dimensional planes. Patran then interpolates between the closed loops to form a bounded three dimensional surface. The surface was then divided into tetrahedra, a uniform mesh size was used throughout and constant density was assumed. Patran performed a three dimensional weighted average based on the volume and the distance to the nearest data point. A "mesh convergence check" was performed, i.e. the elements were tried at a number of different sizes, and the results found to be the same.

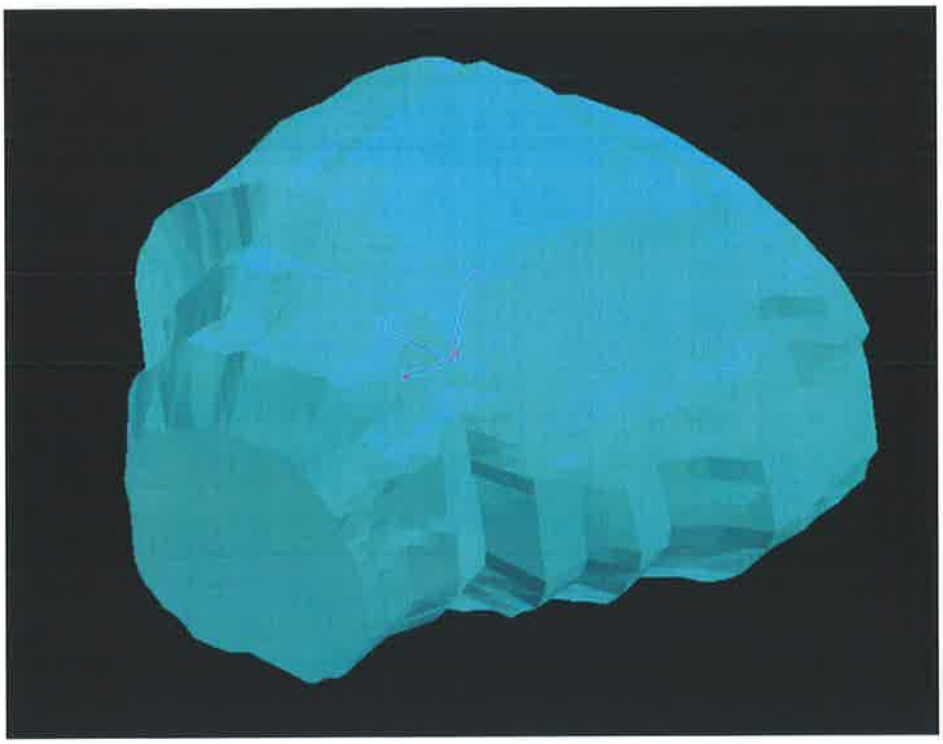

Figure 2: Example of 3D surface generated by Patran showing position of centroid

3.2.1.2 Excel macro

An Excel (Microsoft, Redmond, WA) macro was developed in-house by Dr David Waterhouse. The Excel macro approaches the problem based on the distance to the nearest neighbours on each side of each point. A weighting factor (W_i) is applied to each point (x_i, y_i) which will be lower for closely spaced points and higher for more sparsely spaced points. The weighting factor (W_i) relates to the relative distance (L) between the two nearest points (x_{i-1}, y_{i-1}) and (x_{i+1}, y_{i+1}). The assumption is made that the structure contour is smooth and approximately circular or elliptical. This allows the relative distance (L) to be treated as a chord length. From this the following equations can be defined:

Chord length: $$L_i = \sqrt{(x_{i+1} - x_i)^2 + (y_{i+1} - y_i)^2} \qquad (5.3)$$

Contour perimeter: $$P = \sum_i L_i \qquad (5.4)$$

Weighting factor for point (x_i, y_i): $$W_i = \frac{(L_i + L_{i-1})}{2} \qquad (5.5)$$

So the centre of contour becomes: $x_c = \frac{\sum_i x_i W_i}{L}$ and $y_c = \frac{\sum_i y_i W_i}{L}$ (5.6 and 5.7)

This produces the centre of the contour on each CT slice. These x_c and y_c together with the z_c from the slice position are weighted based on the area of each contour to determine the centroid of the volume.

3.2.1.3 Regular sampling

An IDL (Interactive Data Language - Research Systems, Boulder, CO) code was developed by Dr Martin Ebert. The IDL code uses a different approach to the Excel macro. The structure data points are imported as with the other two methods, then each of the contours on each slice is uniformly sampled on a rectangular grid. This is done by using IDLs "POLYFILLV" routine. The sampling resolution is at a minimum, that of the original CT data set. The centroid and structure volume can then be determined from the number of sample points, slice thickness and resolution.

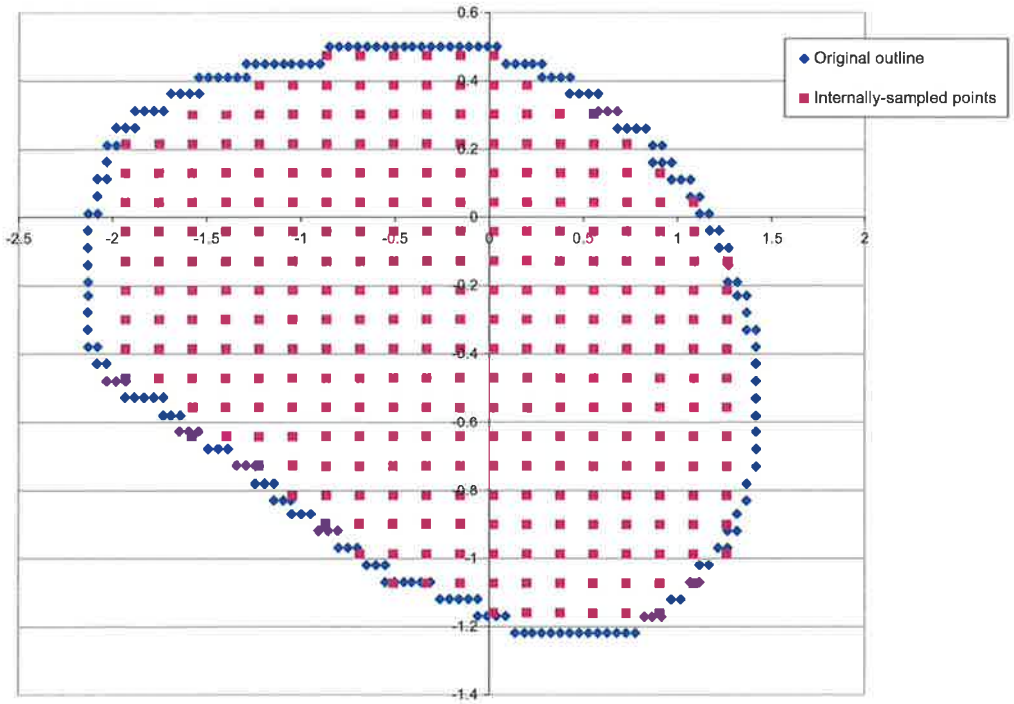

Figure 3: An example of an outline sampled by the IDL code. Example is shown for a lower resolution (20x20) than used for centroid determination (100x100)

The centroid was determined for four contour sets, two prostates and two rectums. These were compared to the finite element model result. The Excel, IDL and XiO determined centroids were compared for all 42 prostate and rectal structures defined.

3.3 Target Delineation

An intra-observer target delineation study was carried out to determine the uncertainty in defining the prostate and the rectum by a single observer. A radiation oncologist was asked on three separate occasions, separated by a minimum of 14 days, to outline the prostate and rectum on two CT scans for each of six patients. The entire prostate as determined by the observer, i.e. the radiation oncologist, was outlined on each consecutive slice. The rectum was defined as by the Trans-Tasman Radiation Oncology Group (TROG) Randomised Androgen Deprivation And Radiotherapy (RADAR) trial protocol as being from the sacro-illiac junction to 1.5cm (5 CT slices) beyond the prostatic apex.

The centroid of each outlined structure was determined using the Excel macro method as described in Section 3.2.1.2. The mean position and standard deviation of the mean position of the prostate and the rectum was determined for each of the CT sets. The root mean square (RMS) of the individual standard deviations was reported as the target delineation uncertainty ($\Sigma_{delineation}$). The volume of both the prostate and the rectum on each of the CT sets, as reported by the RTPS, were also recorded.

Resources, time and radiation oncologists, were not available for an inter-observer variability study and therefore was beyond the scope of this study.

3.4 Method for combining errors to determine appropriate margins

A number of methods for incorporating geometric uncertainties into treatment planning margins have been proposed. Some only consider systematic or random errors in isolation (Bel et al, 1996, Aaltonen et al, 1997). The majority are based on the physical location of the CTV relative to the dose distribution, for example by applying the formula proposed by McKenzie et al (2000) one would expect that the CTV would receive no less than 95% of the prescribed dose for 90% of patients. That is the minimum cumulative dose to the CTV will be 95% of the prescribed dose or greater for 90% of the population (McKenzie et al, 2000). Others have been based on radiobiological response quantifiers, for example the formula proposed by van Herk et al (2000), is based on a 1% tumour control probability (TCP) loss due to geometric uncertainties for the prostate. This margin recipe was designed to give 90% of the population an equivalent uniform dose (EUD) of 98%, for clinically reasonable values of Σ and σ this corresponds with a 1% TCP loss for prostate plans (van Herk, 2004).

For this project the 1% TCP loss margin recipe proposed by van Herk et al (2000) was used. The CTV-PTV margin equation is $2.5\Sigma + 0.7\sigma$ - 3mm, where Σ is the combined systematic geometric uncertainty and σ is the combined random uncertainty (van Herk et al, 2000).

One criticism of this method and others based on biological constraints is that they result in margins that are generally smaller than those calculated by methods based on physical constraints. With this in mind the determined uncertainties will also be used in a margin calculation based on physical considerations. For this purpose the method proposed by McKenzie et al (2000) will be used. The CTV-PTV margin equation is $2.5\Sigma + \beta(\sigma - \sigma_p)$, where Σ is the combined systematic geometric uncertainty, σ is the combined random uncertainty and σ_p is the standard deviation describing the penumbral width (McKenzie et al, 2000).

The value of β accounts for the directional dependency of the penumbra relative to the beam direction, therefore the β used in the equation was chosen for each of the principle axes, based on the beam configuration (McKenzie et al, 2000). The values of β were derived assuming that the beam weights are equal; this introduces a small error (McKenzie et al, 2000). The margin calculations were performed using values for β of 1.15 LR, 1.15 AP and 1.64 SI from Table 1, McKenzie et al (2000). The calculations were performed assuming a 6MV photon beam at a depth of 10cm with a value for the σ_p of 4.5mm. The value of σ_p was estimated from measured profiles. Applying the margin calculated by this method 90% of patients would receive no less than 95% of the prescribed dose to the CTV (McKenzie et al, 2000).

Both of these formulae require the total combined systematic geometric uncertainty (Σ) and the total combined random geometric uncertainty (σ) for a group of patients. In this project not all geometric uncertainties were determined, only the patient specific uncertainties, set-up, organ motion and target delineation, that were the focus of this project were assessed. Hence the CTV-PTV margins calculated, using the values determined and the two methods described above, will only account for those geometric uncertainties.

4 Results

4.1 Set-up accuracy study

Systematic and random set-up errors, for data with (corrected) and without (uncorrected) the application of the patient position protocol described in section 3.1, were calculated.

From the pilot study of 10 patients both systematic and random errors for the uncorrected data were calculated and are shown in Table 3 below.

	LR	AP	SI
$\Sigma_{set\text{-}up}$ (1SD mm)	2.23	3.30	3.86
$\sigma_{set\text{-}up}$ (1SD mm)	2.31	1.99	3.63

Table 3: Uncorrected set-up data for pilot study (n=10)

The errors for the corrected data are shown for comparison in Table 4 below.

	LR	AP	SI
$\Sigma_{set\text{-}up}$ (1SD mm)	0.77	1.19	0.72
$\sigma_{sct\text{-}up}$ (1SD mm)	2.48	2.06	2.79

Table 4: Set-up data for pilot study (n=10) after the application of corrections

With the patient position correction protocol in place the systematic error is reduced considerably and the random error remains relatively unchanged. This is expected as the correction protocol in place at the time of treatment was an offline correction protocol i.e. all corrections are based on information from previous fractions and therefore only reduce the systematic error and not the random error (de Boer et al, 2001).

A mean systematic error ($m_{overall}$) for the group was determined to be -0.76mm LR, -1.05mm AP and 0.07mm SI, for the uncorrected data. Greener (2003) states that assuming the errors follow a normal distribution then this error becomes significant when $m_{overall}$ is greater than $\Sigma_{set\text{-}up}$ divided by the square root of the total number of patients in the group. In this group of patients only the $m_{overall}$ is not significant.

Analysis by de Boer et al (2001) points to small patient studies (N≤10) not being able to provide accurate estimates of $\Sigma_{set\text{-}up}$. In addition to this issue a new CT scanner was introduced into the Department of Radiation Oncology at SCGH. This in turn would result in a different transfer uncertainty between the CT scanner and the RTPS and the CT scanner and the treatment room, which has not been explicitly determined and therefore is included within the set-up errors (McKenzie et al, 2003).

To determine an accurate estimate of $\Sigma_{set\text{-}up}$ further analysis was carried out on a larger group of patients (N=62), whose CT scans were acquired on the new scanner. The distribution of isocentres for both the uncorrected and corrected data is shown in Figure 4 and Figure 5.

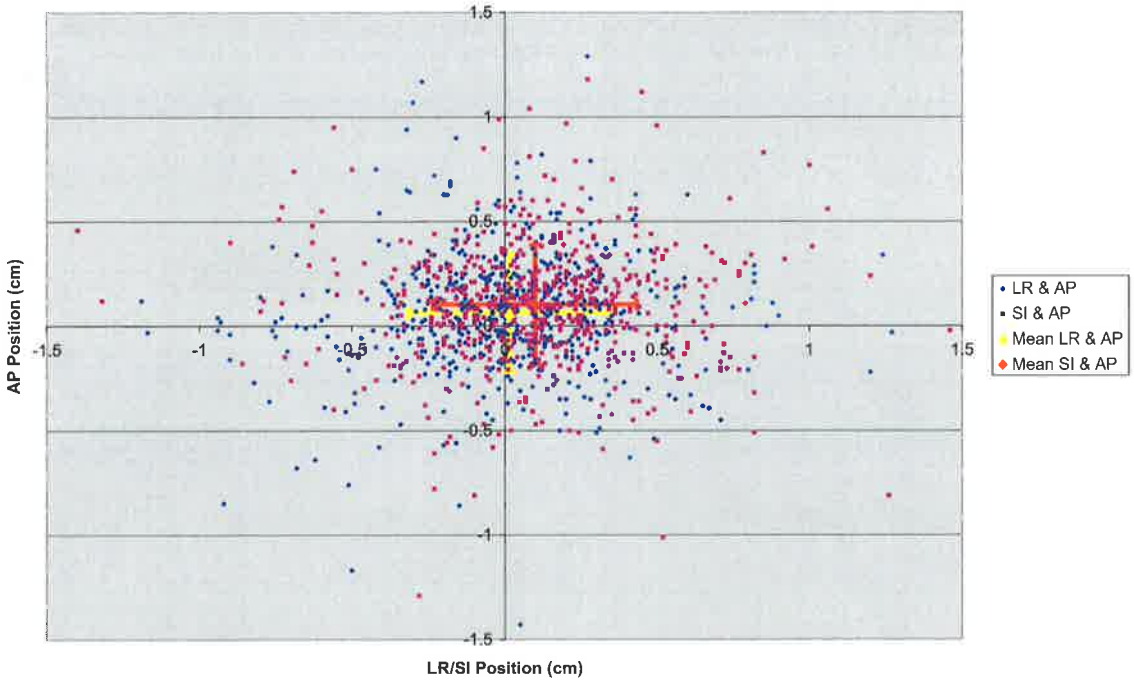

Figure 4: Prostate isocentre positions for the data with no correction protocol applied

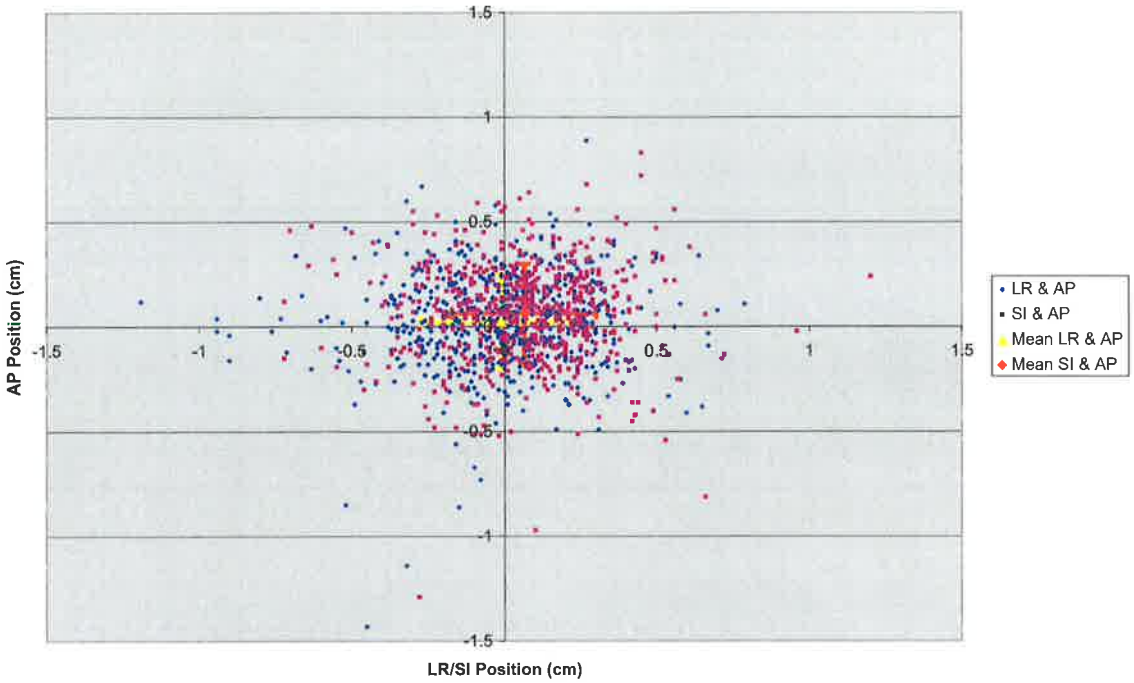

Figure 5: Prostate isocentre positions for the data with the correction protocol applied

The systematic and random set-up errors calculated from these data are shown for both cases in Table 5 and 6 below.

	LR	AP	SI
$\Sigma_{set\text{-}up}$ (1SD mm)	2.54	2.72	1.98
$\sigma_{set\text{-}up}$ (1SD mm)	2.25	2.07	2.03

Table 5: Uncorrected set up uncertainties shown as one standard deviation (mm)

	LR	AP	SI
$\Sigma_{set\text{-}up}$ (1SD mm)	1.57	1.37	1.02
$\sigma_{set\text{-}up}$ (1SD mm)	2.24	2.06	2.00

Table 6: Corrected set up uncertainties shown as one standard deviation (mm)

4.2 Organ motion study

4.2.1 Analysis of methods to determine centre of volume

The centroids as determined by the three test methods were compared to the centroid determined using the finite element model of the structures. The in-house developed IDL code and Excel macro were considered to be superior to XiO in determining the centroid of a structure (assuming the thorough methods employed in Patran provide the most accurate indication of actual centroid position). The results of the analysis for the prostate and the rectum are shown in the Table 7 below.

	Average Difference Relative To Patran					
	Prostate			Rectum		
	LR (mm)	AP (mm)	SI (mm)	LR (mm)	AP (mm)	SI (mm)
XiO	0.3	3.3	-0.6	2.5	0.0	-2.2
Excel	-0.1	-0.4	0.0	0.0	0.9	-0.6
IDL	0.3	-0.4	0.4	0.1	0.9	-0.4

Table 7: Results of centroid determination comparison

As a result of this analysis and access issues to a licensed version of IDL it was determined that the Excel macro would be used for the determination of centroid for this project. Differences in mean positions indicated by each method are approaching the resolution of CT images used in this study (i.e. for a 50cm scan circle pixel size is approximately 0.98 x 0.98 x 3.0 mm). However, only XiO shows differences, in some directions, greater that the resolution of the underlying data. The XiO method of centroid determination simply calculates the centre of the box that bounds the maximum extent of the structure and does not account for the full spatial extent of the volume. Additionally the FEM techniques employed by Patran are known to be rigorous and robust. These factors including the consistency demonstrated between the methods other than XiO, which is known to employ a simplification in its calculation of centroid, formed the basis for the determination that the alternative methods of centroid are superior.

A more extensive analysis of the Excel, IDL and XiO determined centroids was performed. The IDL (n=36) and XiO (n=38) determined centroids for both the prostate and the rectum were compared with that determined by the method used for the project, the Excel macro. Figure 6 and 7 contains a breakdown of the range of deviations in centroid for prostate and rectum respectively.

The average absolute deviation of the IDL determined centroid for the prostate was 0.4mm LR, 0.3mm AP and 0.1mm SI with standard deviations of 0.2mm, 0.2mm and 0.2mm respectively. The average absolute deviation of the XiO determined centroid for the prostate was 0.7mm LR, 1.5mm AP and 4.4mm SI with standard deviations of 0.8mm, 0.9mm and 2.1mm respectively.

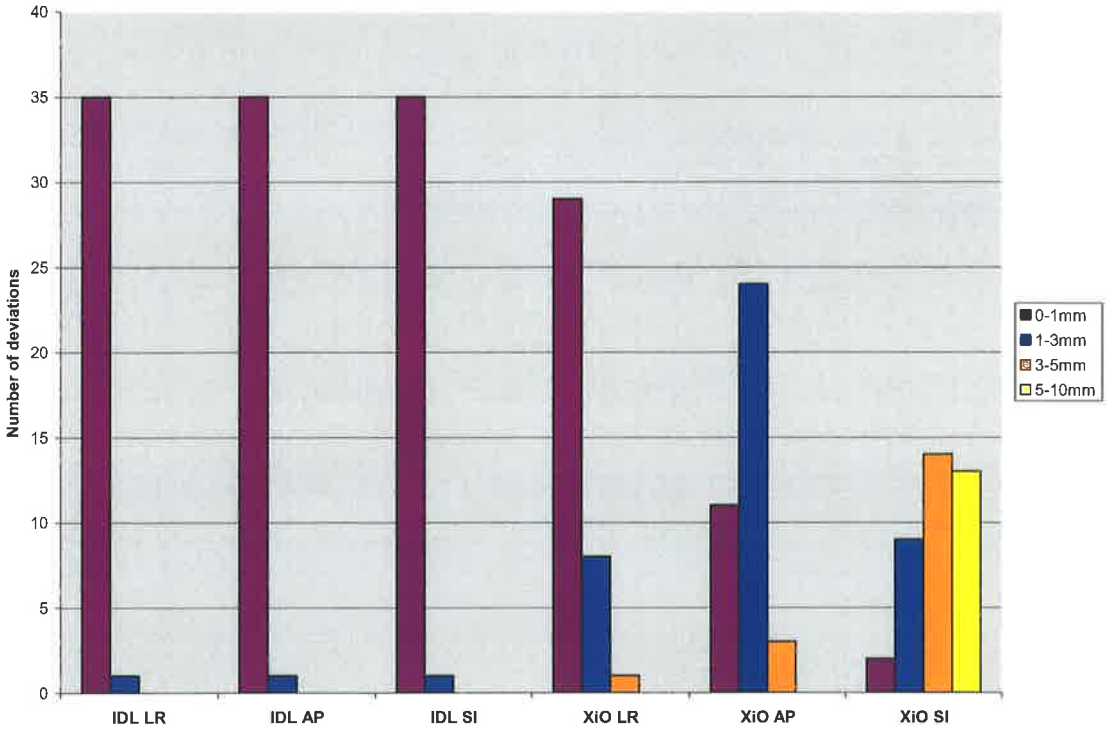

Figure 6: Range of centroid deviations as determined by IDL and XiO relative to Excel marco determination for the prostate

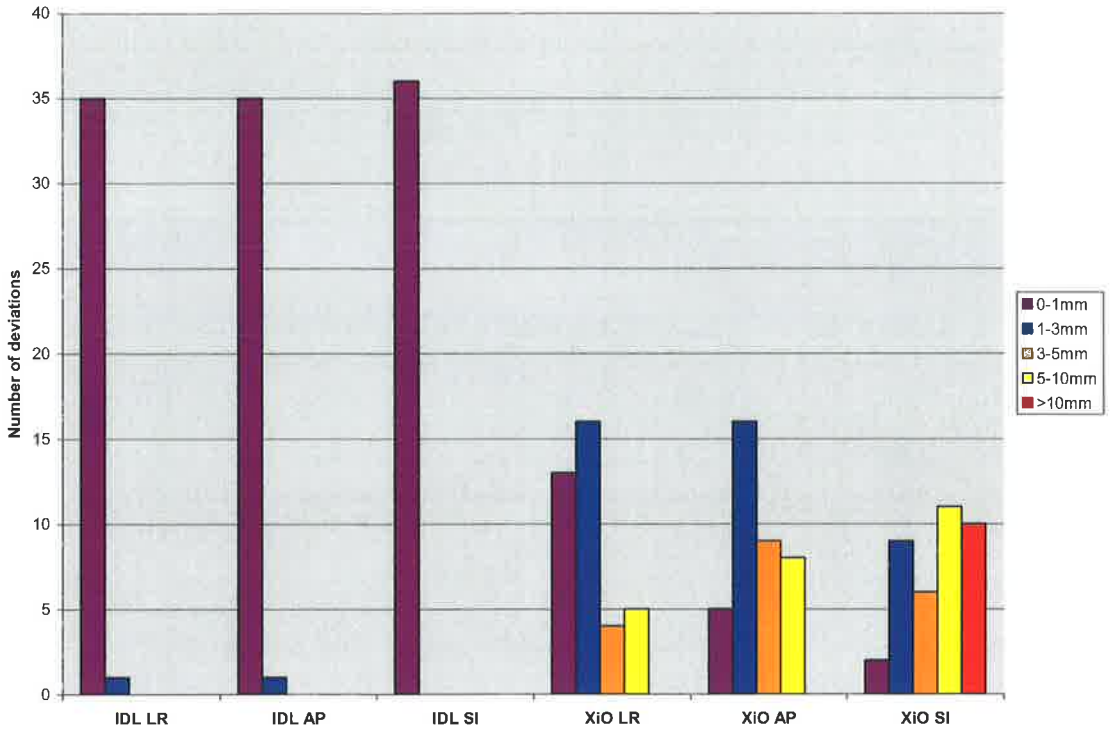

Figure 7: Range of centroid deviations as determined by IDL and XiO relative to Excel marco determination for the rectum

The average absolute deviation of the IDL determined centroid for the rectum was 0.3mm LR, 0.4mm AP and 0.1mm SI with standard deviations of 0.3mm, 0.3mm and 0.1mm respectively. The average absolute deviation of the XiO determined centroid for the rectum was 2.0mm LR, 3.2mm AP and 6.2mm SI with standard deviations of 1.9mm, 2.1mm and 4.1mm respectively.

The uncertainties in centroid position as determined by the XiO RTPS have the potential to underestimate or overestimate organ motion, as the size of the motion being measured is of the order of the errors.

Reported organ motion is via centroid calculations performed with the Excel macro. The reported organ motion includes uncertainties in defining the position of the centroid and intra-observer target delineation.

4.2.2 Organ motion

The organ motion for both the prostate and rectum of each patient and the average for the study group are shown in Figure 8 and Figure 9 below. The majority of prostate motion occurs in the AP and SI directions. The average displacement of the centroid of the prostate for the study group was 0.2mm left, 1.6mm posteriorly and 2.9mm inferiorly. The standard deviations were 1.2mm, 3.1mm and 4.6mm respectively. The average displacement of the centroid of the rectum for the study group was 0.8mm right, 0.6mm posteriorly and 0.7mm inferiorly. The standard deviations were 1.4mm, 3.5mm and 8.3mm respectively.

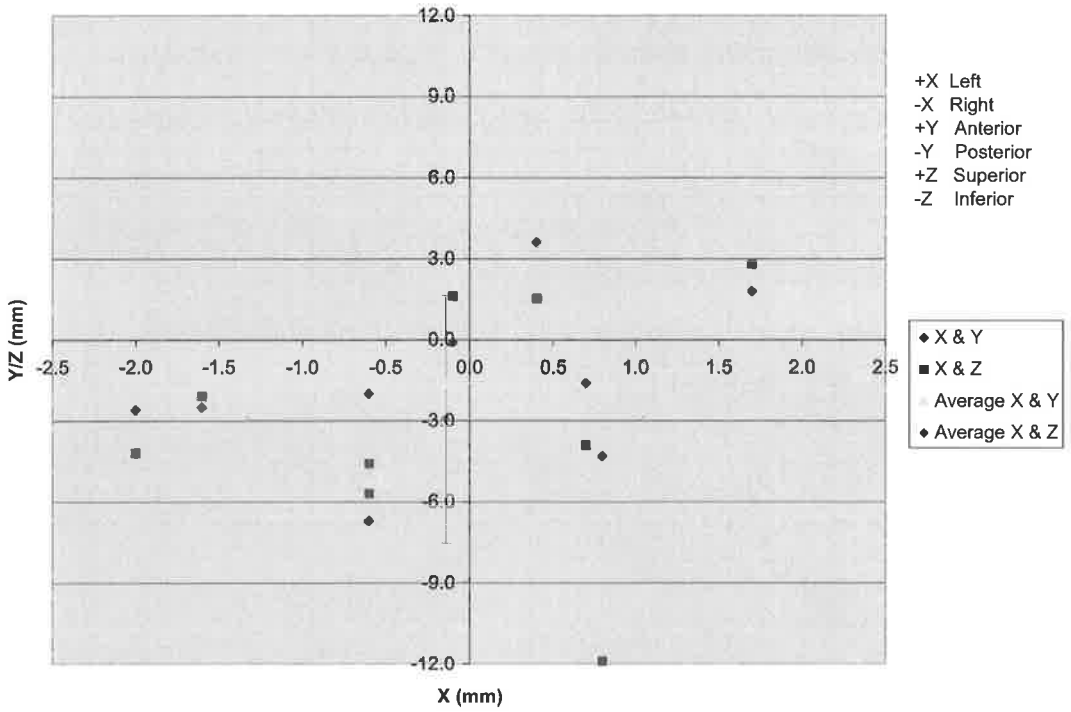

Figure 8: Displacement of the prostate centroids for each individual patient and the average displacement for the study group, relative to the TPCT scan

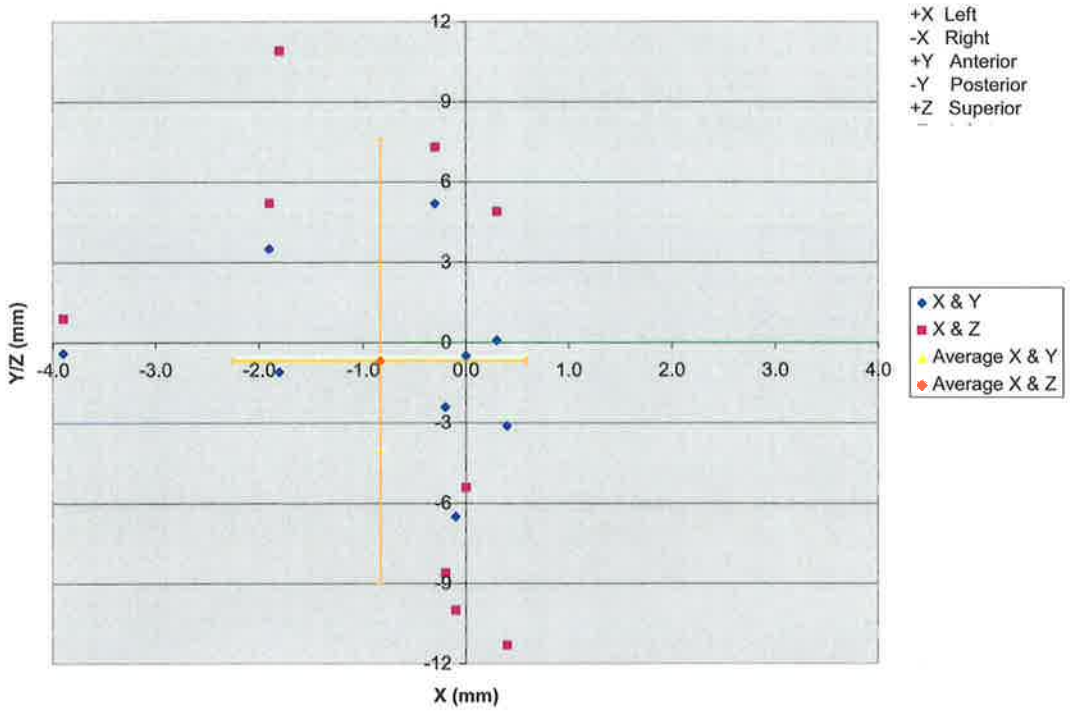

Figure 9: Displacement of the rectum centroids for each individual patient and the average displacement for the study group, relative to the TPCT scan

4.2.3 Factors influencing prostate motion

Prostate motion with respect to fractional change in rectal volume and rectal motion was analysed. The rectal volumes were taken from the XiO RTPS. Parameters that were determined to be significant, p-value <0.05, are shown in Table 9.

The fractional change in rectal volume was found to correlate with prostate motion in each of the three principle directions. The significance of these correlations was tested by means of a t-test. For AP prostate motion a correlation coefficient of 0.6 with a p-value of 0.045 was found, as shown in Figure 10.

The results of the comparison of prostate motion with respect to rectal motion indicate that AP prostate motion correlates with AP and SI rectal motion. Figure 11 shows the relationship between AP prostate motion and SI rectal motion. Additionally, SI motion of the prostate correlates with AP motion of the rectum. The LR motion of the prostate did not correlate with any of the rectal motion directions.

Prostate Parameter	Rectal Parameter	Correlation Coefficient	p-value
AP Prostate Motion	Fvolume Rectum	0.6	0.045
LR Prostate Motion	Fvolume Rectum	0.8	0.009
SI Prostate Motion	Fvolume Rectum	0.6	0.009
AP Prostate Motion	AP Rectal Motion	0.6	0.046
AP Prostate Motion	SI Rectal Motion	0.6	0.033
SI Prostate Motion	AP Rectal Motion	0.8	0.007

Table 8: Correlation of prostate motion with rectal parameters - (Fvolume – fractional change in rectal volume)

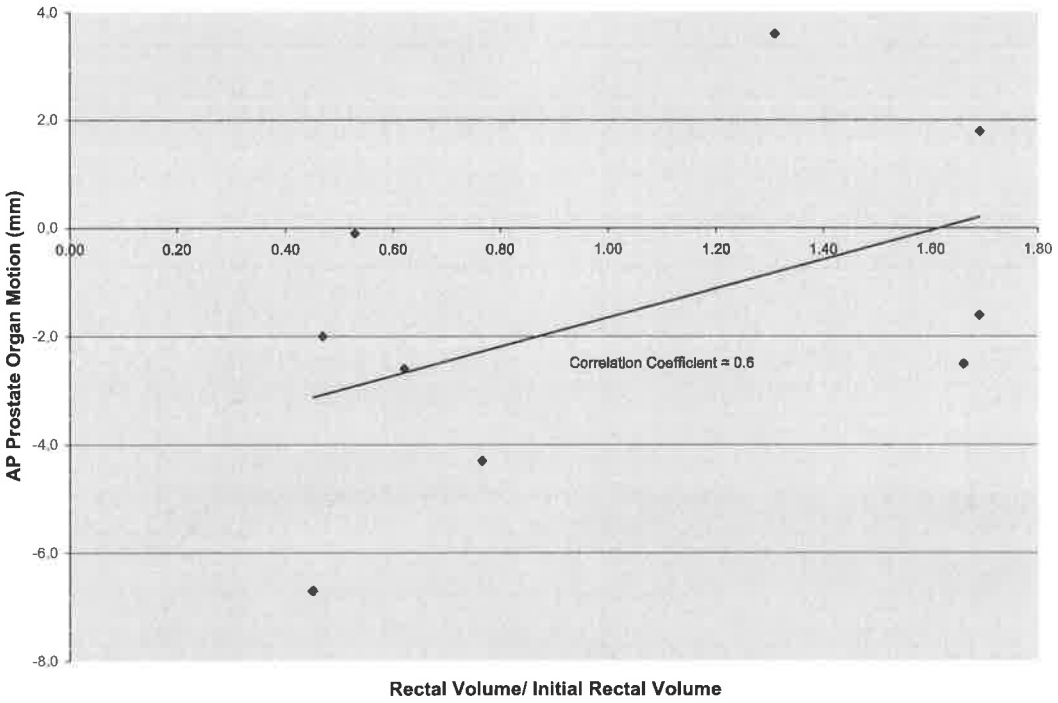

Figure 10: AP prostate organ motion plotted against fractional change in rectal volume (Correlation coefficient 0.6, p-value 0.045)

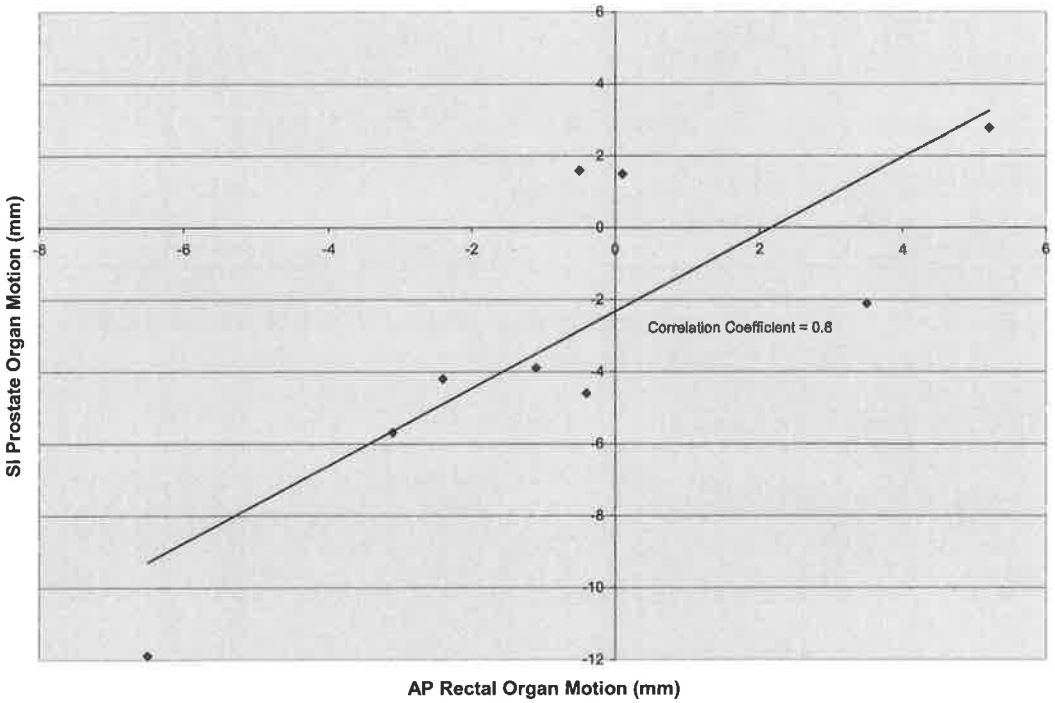

Figure 11: SI prostate organ motion plotted against AP rectal organ motion (Correlation coefficient 0.8, p-value 0.007)

4.3 Target delineation

Six patients had their two CT scans outlined on three separate occasions by a single observer. The average centroid positions and standard deviations were determined for both the prostate and the rectum on each scan, and are summarised in Table 9.

	1 SD (mm)		
	LR	**AP**	**SI**
Prostate CT Scan 1			
1	0.58	1.10	2.50
2	0.16	0.68	0.31
3	0.09	2.15	0.66
4	0.29	1.90	2.25
5	0.44	0.48	0.34
6	0.51	0.29	0.42
Prostate CT Scan 2			
1	0.50	0.23	1.33
2	0.27	0.37	1.67
3	0.42	1.06	1.86
4	0.21	1.25	0.86
5	0.34	0.90	0.89
6	0.31	0.83	1.93
Rectum CT Scan 1			
1	0.26	0.34	1.22
2	0.49	1.68	4.30
3	0.15	0.89	1.25
4	0.56	1.09	2.40
5	0.15	0.46	1.55
6	0.44	1.44	2.21
Rectum CT Scan 2			
1	0.38	0.61	3.11
2	0.39	2.14	5.26
3	0.11	0.41	1.01
4	0.65	2.35	2.59
5	0.12	0.95	1.41
6	0.77	1.57	1.83

Table 9: Standard deviations of structure centroids after multiple delineations

Taking the RMS of the standard deviations results in a target delineation error of 0.37mm LR, 1.10mm AP and 1.45mm SI for the prostate and 0.43mm LR, 1.30mm AP and 2.66mm SI for the rectum.

These values are relatively small compared to the difference in the volumes delineated. The percentage difference in volume delineated relative to the original volume varied from -7.5% to 58.2%, with and average of 10.0%, for the prostate. A similar variation in volumes was seen for the rectum with a range of -22.0% to 56.4%, with an average of 9.8%. No correlation between the percentage change in prostate and rectal volumes was found.

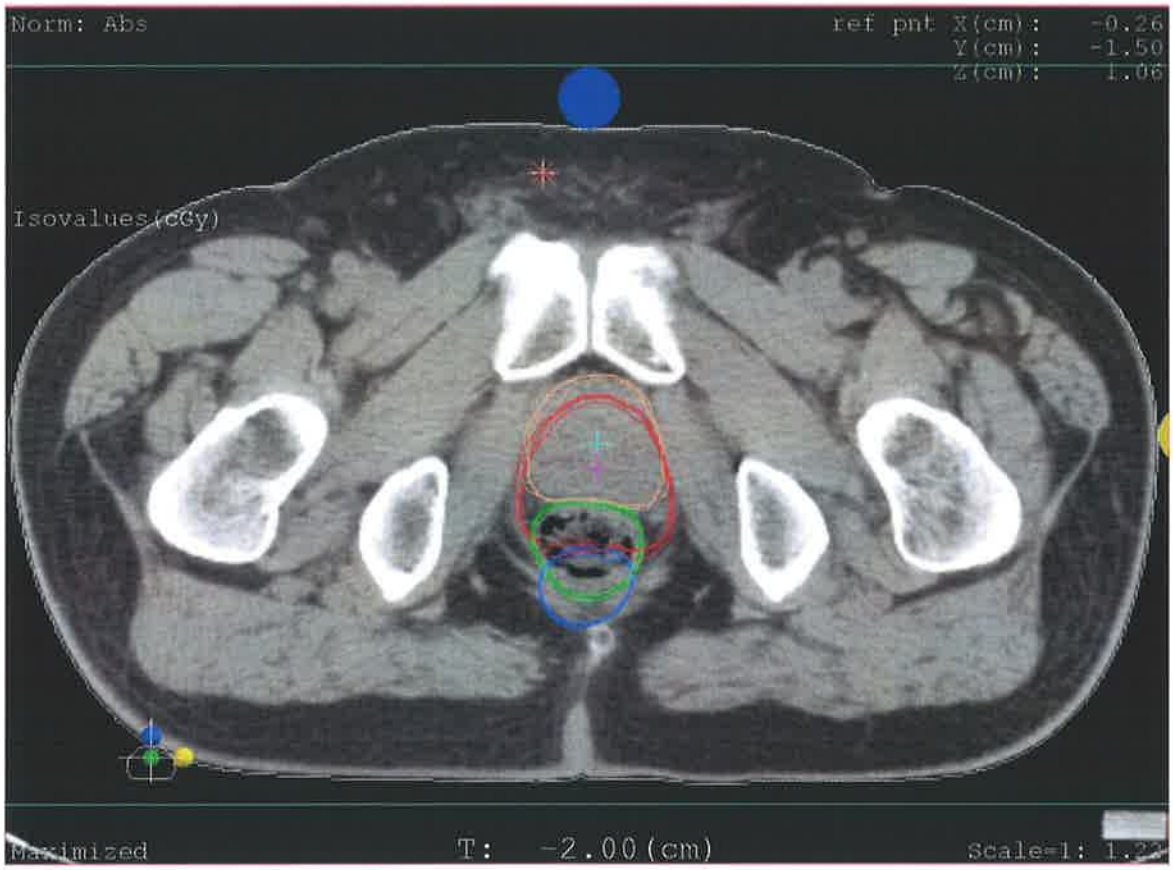

Figure 12: Example of CT slice with contours from both the TPCT and the 2nd CT outlined multiple times

4.4 Combination of uncertainties

The values for set-up uncertainty (with and without the application of the patient position correction protocol) and organ motion uncertainty determined in the sections above will be used for the calculation of a CTV-PTV using the two methods outlines in Section 5.4. Table 10 provides a summary of these values.

	1SD(mm)		
Uncertainty	**LR**	**AP**	**SI**
Uncorrected Random Set-up ($\sigma_{set\text{-}up}$)	2.3	2.1	2.0
Uncorrected Systematic Set-up ($\Sigma_{set\text{-}up}$)	2.5	2.7	2.0
Corrected Random Set-up ($\sigma_{set\text{-}up}$)	2.2	2.1	2.0
Corrected Systematic Set-up ($\Sigma_{set\text{-}up}$)	1.6	1.4	1.0
Organ Motion (Σ_{motion} & σ_{motion})	1.2	3.1	4.6

Table 10: Summary of uncertainties for use in margin calculations

As detailed in Section 3.4 these uncertainties will be used to calculate a CTV-PTV margin using the 1% TCP loss method (van Herk et al, 2000). The results are listed in Table 11 below.

	CTV-PTV Margin (mm)		
	LR	**AP**	**SI**
Uncorrected Set-up Only (σ & Σ)	4.9	5.2	3.4
Corrected Set-up Only (σ & Σ)	2.5	1.9	1.0
Organ Motion Only (σ & Σ)	0.8	6.9	11.7
Uncorrected Set-up & Organ Motion	5.8	9.9	13.0
Corrected Set-up & Organ Motion	3.7	8.1	12.3

Table 11: Margins calculated using data in Table 10 and 1% TCP loss method

The data presented in Table 10 were also used in the calculation of a margin based on physical constraints, i.e. in 90% of cases no part of the CTV will accumulate less than 95% of the prescription dose (McKenzie et al, 2000). The calculations were performed, for simplicity, assuming a 6MV photon beam at a depth of 10cm with a value for the σ_p of 4.5mm, which takes into account the penumbral spread. The value of σ_p was estimated from measured profiles. The results of these calculations are presented in Table 12.

	CTV-PTV Margin (mm)		
	LR	**AP**	**SI**
Uncorrected Set-up Only (σ & Σ)	3.8	4.0	0.9
Corrected Set-up Only (σ & Σ)	1.3	0.6	-1.6
Organ Motion Only (σ & Σ)	-0.8	6.1	11.7
Uncorrected Set-up & Organ Motion	4.8	9.4	13.4
Corrected Set-up & Organ Motion	2.7	7.6	12.6

Table 12: Margins calculated using data in Table 10 and McKenzie et al (2000) method

The negative margin values listed for some scenarios are shown for information only. It is not suggested that negative margins be applied to a CTV to form a PTV.

5 Discussion

Studies of set-up, inter-fraction organ motion and intra-observer uncertainties associated with 3D CRT of the prostate were performed. Tables 13 and 14 summarise the uncertainties determined for the prostate and the rectum.

	LR (mm)	AP (mm)	SI (mm)
Systematic set-up (uncorrected)	2.5	2.7	2.0
Random set-up (uncorrected)	2.3	2.1	2.0
Systematic set-up (corrected)	1.6	1.4	1.0
Random set-up (corrected)	2.2	2.1	2.0
Organ motion	1.2	3.1	4.6
Target delineation	0.4	1.1	1.5

Table 13: Summary of uncertainties determined for the prostate

	LR (mm)	AP (mm)	SI (mm)
Organ motion	1.4	3.5	8.3
Target delineation	0.4	1.3	2.7

Table 14: Summary of uncertainties determined for the rectum

5.1 Set-up accuracy study

Systematic and random uncertainties with and without the application of the patient position correction protocol were determined. The set-up errors calculated were of a similar magnitude to those reported in the literature. The results show that the application of the patient position correction protocol significantly reduced the systematic set-up error whilst having no effect on the random component. This is consistent with the principles of an offline correction protocol.

With the application of the correction protocol the percentage of points within 5mm of the isocentre increased from 88.4% to 95.6%. An example of the influence of

this is patients who are being treated as per the TROG RADAR trial*. As part of the RADAR trial, recommendations on set-up accuracy within specific limits are given for the various certain dose levels, i.e. greater set-up accuracy is recommended for higher prescription doses. For example for a set-up accuracy of 90% or more points within 5mm, the centre may treat with a total dose of up to 74Gy, as opposed to if less than 90% of isocentres are within 5mm then the recommended prescribed dose is 66Gy. This ability to dose escalate safely has been shown for some groups of patients to increase the probability of local tumour control without significant increases in morbidity (Zelefsky et al 1998).

5.2 Organ motion study

The determination of organ motion assumed that organ deformation does not contribute significantly to changes in centroid position. The determination of the centroid is limited by resolution of the RTOG-exported data. The structure coordinates have a resolution of 0.4mm in the LR and AP directions, and the resolution in the SI direction is limited by the CT slice spacing which was 3mm. This results in a centroid calculation with a minimum resolution of 0.2mm LR and AP and 1.5mm SI.

Organ motion was shown to be greater in the AP and SI directions. The results of prostatic organ motion for this study are similar to other studies published in the literature. Figure 13 shows the results of this study relative to other published series. Table 15 contains brief descriptions of the series.

* TROG trial 03.04 - http://www.ranzcr.edu.au/affiliatedgroups/trog/index.cfm

Serie	Description	LR (1SD mm)	AP (1SD mm)	SI (1SD mm)
This Study	2 CT Scans; No rectal filling protocol; Bladder "comfortably full"; Supine; Motion of centroid assessed	1.2	3.1	4.6
Dawson et al (1998)	Weekly CT; Empty bladder; Supine; motion estimated by removing set-up error from total position variability	1.8	2.2	2.5
Tinger et al (1998)	Weekly CT; No rectal filling protocol; Full bladder; Supine; Motion of centre of mass assessed	0.9	2.6	3.9
Roeske et al (1995)	Weekly CT; Full bladder; Supine; Motion of centre of mass assessed	0.7	3.9	3.2
Antolak et al (1998)	4 CT scans; Full bladder; Supine; Motion of centre of mass assessed	0.9	4.1	3.6

Table 15: Details of prostate motion studies

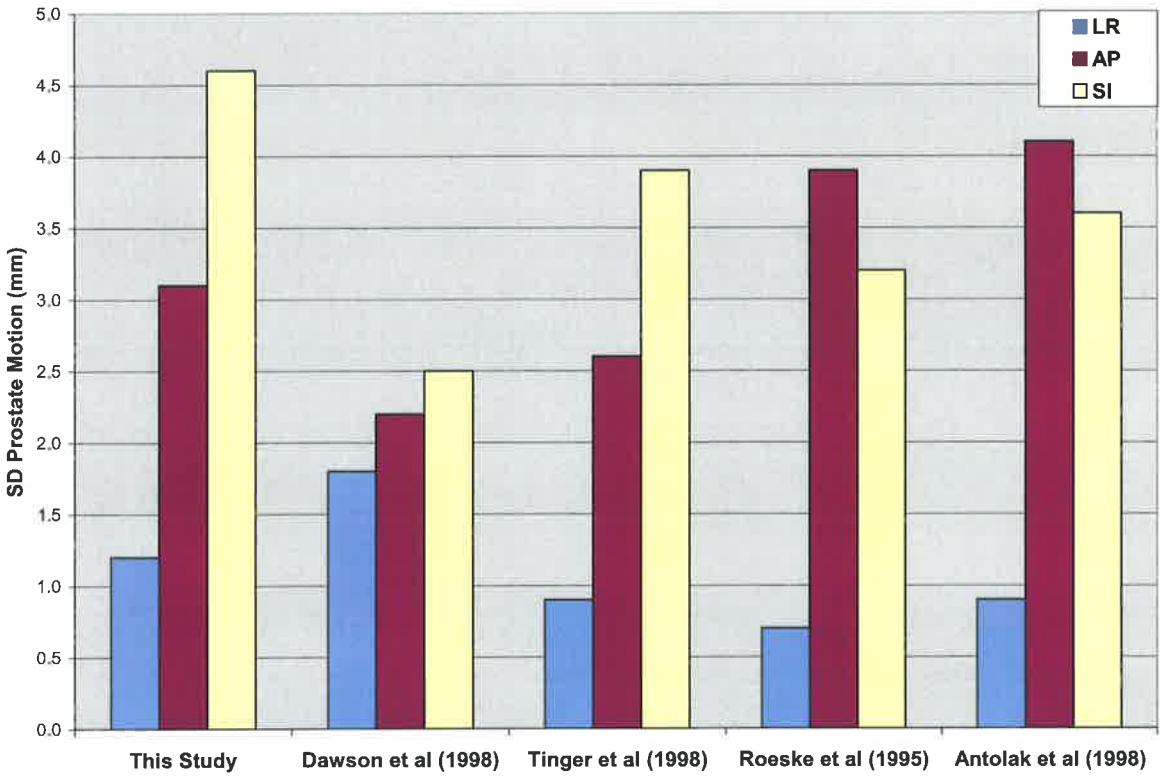

Figure 13: Standard deviations of prostate motion studies

The state of the rectum was shown to be an important factor in the motion of the prostate. The fractional change in rectal volume was shown to correlate with

prostate motion in the three cardinal directions. The AP motion of the prostate correlated with the AP and SI rectal motion and the SI motion of the prostate correlated with the AP rectal motion. This result is similar to that found by Tinger et al (1998), who found the motion of the prostate in the AP direction correlated with the fractional change in rectal volume (r-0.6). For LR and SI prostate motion the correlation coefficients were 0.8 and 0.6 with p-values of 0.009 and 0.040 respectively.

5.3 Target delineation

Intra-observer target delineation uncertainty was assessed and found to be largest in the SI direction for both the prostate and the rectum; 1.45mm and 2.66mm (1 SD) respectively. $\Sigma_{delineation}$ was determined to be sub-millimetre in the LR direction. This analysis was only able to provide an estimate of the $\Sigma_{delineation}$ as the structures were only outlined three times each. To obtain a statistically significant measurement of the intra-observer delineation uncertainty would require more than 3 repeat delineations, however resources were not available for such an extensive study.

It does however indicate that the target delineation errors are larger in both the AP and SI directions. There are a number of potential sources accounting for the increased uncertainty in these two directions. One potential source of uncertainty is the difficulty in defining the prostate using CT. Remeijer P et al (1999) found that intra-observer variation was largest near the seminal vesicles and the apex. They also found that systematic observer variation was largest near the caudal-anterior side of the prostate (Remeijer et al, 1999). Another potential source of uncertainty is the partial volume effect related to CT slice spacing. This effect is more prominent at the apex of the prostate where the size of the prostate is changing rapidly relative to the size of the CT slices (Livesy et al, 2004).

5.4 Combination of uncertainties

The CTV-PTV margins calculated, with the set-up and organ motion uncertainty determined in this study, by both the van Herk et al (2000) and the McKenzie et al (2000) methods yielded similar results. Both methods predict that the CTV-PTV margin should be greatest in the SI direction and smallest in the LR direction. Organ motion uncertainty, whose values determined in this project include target delineation uncertainty, is the largest contributor to the margins calculated by these methods. The data presented in this thesis is applicable for patients treated at Sir Charles Gairdner Hospital using the processes described in section 2.6 and do not account for inter-observer variability in organ delineation or inter- and intra observer variability in image matching. For these patients with the application of the patient positioning protocol a CTV-PTV margin was calculated using the van Herk et al (2000) method the McKenzie et al (2000) method and values are shown in Table 16.

Method	LR (mm)	AP (mm)	SI (mm)
Van Herk et al (2000)	3.7	8.1	12.3
McKenzie et al (2000)	2.7	7.6	12.6

Table 16: Summary of CTV-PTV margins calculated

At the time the patient's on this study were treated a common choice of CTV-PTV margin was 10mm in all directions except posteriorly which was 5mm, this formed the phase 1 target volume PTV1. For phase 2 the margins were reduced to 6mm in all directions except posteriorly where the margin was reduced to zero. The size of the actual margins applied was limited by resolution of the structure expansion algorithm. Comparing these margins to those determined in this study, the clinically applied margins would appear to be inadequate for the posterior, superior and inferior margins for phase 1 and in all directions for phase 2. In some cases it is not practical to increase the CTV-PTV margin, for example posteriorly where it can extend into the rectum, which is an organ at risk.

Studies have shown that increasingly conformal and IMRT treatments with dose escalation have resulted in increased local control of the tumour (Zelefsky et al, 1998). One interpretation of these studies is that the increase in margins suggested by the calculations in this study may not be necessary. However the uncertainties associated with these patients are real. The literature suggests that using reduced margins does not impact on local control when used with dose escalation. This could be because the higher prescribed dose compensates for the volumes of tissue that are potentially underdosed due to organ motion or set-up uncertainty, or, because the CTV marked on CT is typically larger than the true prostate volume. There are a number of uncertainties which are related to this imaging modality. One is the partial volume effect, as previously mentioned this effect increases in severity when the target changes size rapidly relative to the CT slice spacing. This can make the apex of the prostate difficult to define. Another reported disadvantage of CT is that the volume of the prostate defined on CT is consistently larger than that on MRI. Rasch et al (1999) found that in 96% of cases the volume delineated on CT was larger than the volume delineated on MRI, with an average CT to MRI volume ratio of 1.4. The CT derived apex was on average 6mm larger than on MRI (Rasch et al, 1999). Roach et al (1996) found similar results with the average CT prostate volume being 32% larger than the MRI volume. The average maximum discrepancy was 7mm posteriorly and 4.5mm in the inferior apical prostate (Roach et al, 1996). It may be possible that the inherent target delineation uncertainty in CT imaging, which results in larger volumes than MRI, unwittingly counteracts the smaller, clinically applied margins.

Recommendations from this study for reducing CTV-PTV margins from those calculated in this study include the use of MRI fused with CT for delineation of the CTV. Prior to reducing margins an assessment of organ motion and target delineation using MRI is required. Changing from an offline correction protocol to an online correction protocol will reduce the random set-up uncertainty; however this uncertainty is a smaller contributor to the required CT-PTV margin compared with organ motion and target delineation. A method of localising the prostate on a daily basis, by ultrasound or implanted markers for example, has the potential to reduce the geometric uncertainties involved.

6 Conclusion

Set-up, organ motion and intra-observer target delineation uncertainties were determined for patients undergoing 3D CRT of the prostate at Sir Charles Gairdner Hospital, Perth, Western Australia.

Systematic and random uncertainty was determined by a study of 62 patients with an average of 10 electronic portal images. The analysis was performed by the matching of bony anatomy on the EPI to a reference DRR. The use of an offline patient correction protocol was shown to reduce the systematic component of set-up error. The systematic set-up uncertainty (1 SD), after the application of the patient correction protocol, was 1.57mm LR, 1.37mm AP, 1.02mm SI and the random component was 2.24mm LR, 2.06mm AP, 1.02mm SI.

Organ motion for the prostate and the rectum was determined by the change in structure centroid between CT scans. A number of methods were analysed to accurately determine the structure centroids. The centroid as determined by the planning system was determined to be insufficiently accurate for use in detecting the size of movements expected. An Excel macro was developed and used to calculate the centroids that were subsequently used to determine both organ motion and intra-observer target delineation. The Excel macro produced accurate centroids that were within the resolution of the CT image, compared to a finite element model determined centroid.

Organ motion and target delineation errors were found to be largest in the SI direction and smallest in the LR direction. Prostate organ motion was found to correlate with the fractional change in rectal volume. Organ motion uncertainty (1 SD) of the prostate was 1.2mm LR, 3.1mm AP, 4.6mm SI and 1.4mm LR, 3.5mm AP, 8.3mm SI for the rectum.

From these uncertainties CTV-PTV margins were calculated using two methods. The margin methods yielded similar results. The larger margin in the SI direction is consistent with the increased uncertainty in defining the inferior extent of the

prostate on a transverse CT scan. The CTV-PTV margin calculated using the physical constraint model (McKenzie et al, 2000) was 2.7mm LR, 7.6mm AP, 12.6mm SI and the biological constraint model (van Herk et al, 2000) resulted in a margin of 3.7mm LR, 8.1mm AP, 12.3mm SI.

The values for the uncertainties determined in the study were consistent with previously published series. The effectiveness of an offline set-up correction protocol to reduce systematic set-up errors was shown, and the larger uncertainties of organ motion and target delineation were determined. These uncertainties have been shown to be significant and require consideration when reducing margins. A CTV-PTV margin was calculated which will account for these uncertainties.

Potential areas of further investigation include dosimetric analysis of the effects of these uncertainties. Plans could be generated to produce dose volume histograms for analysis and for estimating outcome effects. From these plans normal tissue complication probabilities and tumour control probabilities could be calculated. Another area of further study is the clinical follow-up of patients that are routinely treated with CTV-PTV margins smaller than those calculated in this study. An assessment could be carried out to assess what, if any, effect these uncertainties have on outcome. A further investigation into organ motion and target delineation could be carried out using MRI as opposed to CT as the imaging modality.

7 Appendices

7.1 List of Abbreviations

3DCRT	Three Dimensional Conformal Radiotherapy
ABS	Australian Bureau of Statistics
ADHT	Androgen deprivation hormonal therapy
AP	Anterior/Posterior
CT	Computerised Tomography
CTV	Clinical Target Volume
DRR	Digitally Reconstructed Radiograph
EBRT	External Beam Radiotherapy
EPI	Electronic Portal Imaging
EUD	Equivalent Uniform Dose
GTV	Gross Target Volume
ICRU	International Commission of Radiation Units
IMRT	Intensity Modulated Radiotherapy
LAN	Local Area Network
LR	Left/Right
MRI	Magnetic Resonance Imaging
OR	Organ at Risk
PSA	Prostate Specific Antigen
PTV	Planning Target Volume
RADAR	Randomised Androgen Deprivation and Radiotherapy
RMS	Root Mean Square
RTOG	Radiation Therapy Oncology Group
RTPS	Radiotherapy Treatment Planning System
SCGH	Sir Charles Gairdner Hospital
SD	Standard Deviation
SI	Superior/Inferior
TCP	Tumour Control Probability
TPCT	Treatment Planning Computerised Tomography
TROG	Trans-Tasman Radiation Oncology Group

7.2 RTOG Data Format

The RTOG data exchange format was developed by the RTOG 3D QA Center (now the Image Guided Therapy Center at Washington University). It was based on Report Number 10 of the American Association of Medical Physicists (Baxter et al, 1982).

This data format includes all radiographic data for a patient as well as 3D dose distributions, treatment field definitions and any calculated dose volume histograms. Of relevance to this project were the structure files representing delineated organ contours. The structure files generated by the RTOG Data Submission function are in ASCII format. The contours are grouped by CT slice, and although it is not necessary for each CT slice to have a contour it is necessary that all slices with a contour are adjoining (Bosch W, 1999). Following is the data that is contained within a RTOG structure file (Bosch W, 1999):

Number of levels (total # of scans)
Scan number (=1 for first scan, etc.)
Number of segments in this level (scan)
Number of points in first segment
Triplets of (x, y, z) coordinates, one per point, last=first
Number of points in second segment
Triplets of (x, y, z) coordinates, one per point, last=first

This listing of scans segments and triplets of coordinates continues for the length of the entire CT scan.

7.3 International Commission of Radiation Units and Measurements (ICRU) Reports 50 and 62 Definitions

The margins added to the clinical target volume (CTV) are designed to account for these uncertainties in order to avoid not only a geographical miss but to limit unwanted dose to any organs at risk (OAR). ICRU 50 and 62 define the various volumes involved. The volumes of interest in this project are defined and illustrated in Table 17 and Figure 14 below.

Gross Tumour Volume (GTV)	The macroscopic extent of the tumour mass. Clinically identifiable by physical examination, endoscopy and imaging modalities.
Clinical Target Volume (CTV)	The CTV is an extension of the GTV to include a margin around the GTV to take into account the probability of the presence of microscopic extension of the tumour beyond the GTV.
Planning Target Volume (PTV)	Takes into account the uncertainties due to patient movement, patient to beam positioning, and radiotherapy equipment. This is expanded in ICRU Report 62 to be made up of an internal margin (IM) and a set-up margin (SM). CTV+IM+SM = PTV.
Internal Margin (IM)	Takes into account changes in the shape size and position of the CTV during a course of treatment
Set-up Margin (SM)	Takes into account uncertainties in the patient to beam positioning
Organ At Risk (OR)	Is normal tissue whose proximity to the CTV and radiosensitivity may limit treatment planning and/or absorbed dose level.

Table 17: ICRU definitions (ICRU Report 62)

Figure 14: Diagram representing relationship between the GTV, CTV and PTV

7.4 Raw Set-up Data

Patient Number	Isocentre Position (mm)			Isocentre Shift (mm)		
	LR	AP	SI	LR	AP	SI
Patient 1	-0.20	-0.23	-0.31	0	0	0
	-0.11	-0.10	-0.84	0	0	0
	-0.19	-0.27	-0.23	0	0	0
	-0.04	-0.40	-0.22	0	0	0
	0.05	-0.31	-0.19	0	0	0
	0.02	-0.15	-0.21	0	0	0
	-0.14	0.00	-0.25	0	0	0
	0.18	-0.15	0.09	0	0	0
	0.03	-0.28	-0.57	0	0	0
	-0.10	-0.20	-0.49	0	0	0
	-0.13	-0.31	0.18	0	0	0.5
	-0.04	-0.35	0.13	0	0	0
	0.02	-0.33	0.27	0	0	0
	-0.07	-0.19	0.04	0	0	0
	0.02	-0.33	0.22	0	0	0
	0.04	-0.34	0.16	0	0	0
	-0.17	-0.26	-0.10	0	0	0
	-0.29	-0.26	-0.11	0	0	0
	-0.01	0.07	0.56	0	0	0
	-0.44	-0.23	-0.02	0	0	0
	-0.01	-0.22	0.36	0	0	0
	0.16	-0.10	0.01	0	0	0
	-0.01	0.00	0.66	0	0	0
	0.23	-0.40	0.30	0	0	0
	-0.38	-0.76	0.21	0	0	0
	-0.04	-0.35	0.08	0	0	0
	-0.41	-0.21	0.55	0	0	0
	0.14	-0.06	0.35	0	0	0
Patient 2	0.29	0.06	0.75	0	0	0
	0.02	0.06	0.29	0	0	0
	0.11	-0.09	-0.17	0	0	0
	0.06	-0.32	-0.01	0	0	0
	0.43	-0.18	0.14	0	0	0
	0.10	0.11	0.17	0	0	0
	-0.16	-0.03	0.46	0	0	0
	0.07	-0.23	0.24	0	0	0
	-0.10	-0.32	0.16	0	0	0
	-0.13	0.19	0.21	0	0	0
	0.29	0.10	-0.01	0	0	0
	-0.15	0.06	0.21	0	0	0
	0.01	0.00	0.00	0	0	0
	0.03	-0.17	-0.58	0	0	0
	0.18	-0.05	-0.35	0	0	0
	0.23	-0.21	-0.06	0	0	0
	0.14	0.11	0.25	0	0	0
	-0.14	-0.16	-0.15	0	0	0

Patient Number	Isocentre Position (mm)			Isocentre Shift (mm)		
	LR	AP	SI	LR	AP	SI
Patient 2	-0.11	-0.37	0.23	0	0	0
	0.16	-0.29	0.03	0	0	0
	0.10	-0.37	0.01	0	0	0
	0.30	0.00	0.21	0	0	0
	0.22	-0.04	-0.04	0	0	0
	0.20	-0.13	0.28	0	0	0
	0.11	-0.16	-0.06	0	0	0
Patient 3	-0.14	-0.21	-0.40	0	0	0
	0.17	0.21	-0.36	0	0	0
	-0.05	0.11	-0.43	0	0	0
	0.19	-0.08	-0.39	0	0	0
	0.26	0.14	-0.40	0	0	0
	-0.01	0.00	0.07	0	0	0
	-0.02	0.03	-0.32	0	0	0
	-0.04	0.05	-0.11	0	0	0
	0.09	0.15	0.18	0	0	0
	-0.13	-0.05	2.25	0	0	0
	0.43	0.00	0.16	0	0	0
	-0.33	0.06	0.51	0	0	0
	-0.13	0.02	0.19	0	0	0
	-0.35	0.20	0.06	0	0	0
	-0.18	0.10	0.00	0	0	0
	-0.18	0.21	0.17	0	0	0
	-0.22	0.03	0.29	0	0	0
	0.19	0.13	0.27	0	0	0
	-0.92	0.00	0.06	0	0	0
	-0.77	0.09	-0.26	0	0	0
	-0.10	0.16	0.23	0	0	0
	-0.23	-0.36	0.26	0	0	0
	-0.96	0.10	-0.21	0	0	0
	0.21	0.18	0.10	0	0	0
	0.13	0.11	0.23	0	0	0
	0.17	0.10	0.07	0	0	0
	-0.40	0.16	0.11	0	0	0
	0.24	-0.07	-0.08	0	0	0
	-0.01	0.10	-0.01	0	0	0
	-0.06	0.17	0.73	0	0	0
Patient 4	-0.17	0.06	-0.08	0	0	0
	-0.02	0.07	-0.31	0	0	0
	-0.40	-0.21	-0.45	0	0	0
	-0.06	0.00	0.04	0	0	0.4
	-0.03	0.12	0.08	0	0	0
	-0.32	0.06	0.40	0	0	0
	-0.18	-0.05	0.28	0	0	0
	-0.27	0.06	-0.09	0	0	0
	-0.02	0.06	0.28	0	0	0

Patient Number	Isocentre Position (mm)			Isocentre Shift (mm)		
	LR	AP	SI	LR	AP	SI
Patient 4	-0.19	-0.05	0.30	0	0	0
	-0.25	-0.05	0.24	0	0	0
	-0.19	-0.17	0.39	0	0	0
	-0.13	0.12	0.21	0	0	0
	-0.11	-0.10	0.05	0	0	0
	-0.26	-0.12	0.40	0	0	0
	-0.30	0.00	0.30	0	0	0
	-0.29	0.05	0.32	0	0	0
	0.05	0.00	-0.05	0	0	0
	-0.10	-0.14	-0.15	0	0	0
	-0.17	-0.10	-0.12	0	0	0
	-0.25	0.17	-0.15	0	0	0
	-0.11	0.12	-0.13	0	0	0
	-0.02	0.12	-0.07	0	0	0
	0.18	0.13	-0.17	0	0	0
	-1.26	0.07	-0.16	0	0	0
	0.03	0.23	-0.17	0	0	0
	-0.23	0.05	0.48	0	0	0
	-0.04	-0.08	0.01	0	0	0
	-0.05	0.12	-0.01	0	0	0
	-0.16	0.14	-0.12	0	0	0
	0.19	0.10	-0.27	0	0	0
	0.20	-0.02	-0.12	0	0	0
	0.05	-0.10	-0.10	0	0	0
Patient 5	-0.02	0.10	0.37	0	0	0
	0.02	0.00	0.79	0	0	0
	-0.43	-0.15	0.11	0	0	-0.5
	0.48	0.15	0.26	0	0	0
	-0.09	-0.05	0.35	0	0	0
	0.52	-0.06	0.41	0	0	0
	-0.14	-0.19	0.11	0	0	-0.3
	-0.16	0.13	0.25	0	0	0
	-0.18	-0.15	0.01	0	0	0
	0.14	0.11	0.12	0	0	0
	-0.31	0.03	-0.01	0	0	0
	-0.06	0.08	0.03	0	0	0
	-0.14	-0.03	-0.11	0	0	0
	-0.14	-0.35	0.28	0	0	0
	-0.23	0.15	0.15	0	0	0
	-0.17	-0.14	0.34	0	0	0
	0.19	0.33	0.05	0	0	0
	-0.30	0.08	0.17	0	0	0
	0.06	-0.05	-0.09	0	0	0
	0.37	0.11	0.04	0	0	0
	-0.07	0.00	0.06	0	0	0
	-0.17	0.08	0.10	0	0	0

Patient Number	Isocentre Position (mm)			Isocentre Shift (mm)		
	LR	AP	SI	LR	AP	SI
Patient 5	-0.11	-0.15	0.00	0	0	0
	-0.07	-0.17	-0.10	0	0	0
	-0.07	0.06	0.23	0	0	0
	0.11	0.00	0.01	0	0	0
	-0.19	0.06	-0.09	0	0	0
	0.44	0.00	-0.01	0	0	0
Patient 6	0.41	-0.44	-0.54	0	0	0
	-0.12	-0.05	-0.16	0	0	0
	0.33	-0.44	-0.13	0	0	0
	-0.06	-0.38	-0.32	0	0	0
	-0.13	-0.16	-0.13	0	0	0
	0.11	0.50	-0.39	0	0	0
	0.17	-0.15	-0.14	0	0	0.3
	0.35	-0.23	-0.21	0	0	0
	0.16	-0.33	0.07	0	0	0
	-0.14	-0.10	-0.15	0	0	0
	-0.32	-0.35	0.04	0	0	0
	-0.01	-0.40	-0.01	0	0	0
	0.10	0.15	-0.16	0	0.3	0
	0.03	0.13	-0.04	0	0	0
	-0.12	0.15	-0.12	0	0	0
	-0.15	0.24	-0.25	0	0	0
	-0.10	0.01	-0.06	0	0	0
	-0.27	0.02	-0.20	0	0	0
	0.11	0.04	-0.53	0	0	0
	-0.06	-0.02	0.11	0	0	0.3
	0.02	0.09	0.45	0	0	0
	-0.11	0.07	0.06	0	0	0
	-0.24	0.13	0.52	0	0	0
	0.08	0.16	0.31	0	0	0
	0.05	0.16	0.44	0	0	0
	0.31	0.09	0.27	0	0	0
	-0.04	0.28	0.37	0	0	0
	0.05	0.21	0.19	0	0	0
	0.16	-0.02	0.27	0	0	0
	-0.41	-0.08	0.12	0	0	0
Patient 7	-0.08	0.58	-0.04	0	0	0
	-0.08	0.45	-0.20	0	0	0
	-0.08	0.71	0.13	0	0	0
	-0.30	0.05	0.26	0	-0.5	0
	0.27	-0.33	-0.36	0	0	0
	-0.31	0.11	-0.05	0	0	0
	-0.12	0.11	0.01	0	0	0
	-0.01	0.40	0.38	0	0	0
	0.13	0.31	0.07	0	0	0
	0.16	0.65	0.61	0	0	0

Patient Number	Isocentre Position (mm)			Isocentre Shift (mm)		
	LR	AP	SI	LR	AP	SI
Patient 7	0.08	0.39	0.17	0	0	0
	-0.07	-0.19	0.06	0	-0.4	0
	0.10	0.25	0.02	0	0	0
	-0.14	0.36	-0.01	0	0	0
	-0.16	0.22	-0.13	0	0	0
	-0.11	0.13	0.30	0	0	0
	0.01	0.02	-0.19	0	0	0
	-1.46	-0.06	0.04	0	0	0
	0.18	-0.01	0.06	0	0	0
	0.20	0.26	-0.07	0	0	0
	0.08	0.09	-0.10	0	0	0
	-0.31	0.31	0.09	0	0	0
	-0.25	-0.22	-0.05	0	0	0
	-0.16	0.08	-0.05	0	0	0
	-0.27	0.22	0.06	0	0	0
	-0.66	0.40	0.23	0	0	0
	0.11	0.02	0.14	0	0	0
	0.19	0.20	0.10	0	0	0
	0.04	-0.11	-0.02	0	0	0
Patient 8	-0.56	-0.02	-0.65	0	0	0
	-0.59	-0.35	-0.42	0	0	0
	0.19	0.03	0.13	0.5	0	0.4
	-0.03	-0.09	-0.09	0	0	0
	-0.32	0.37	-0.02	0	0	0
	0.16	0.24	0.10	0	0	0
	-0.33	0.25	-0.18	0	0	0
	-0.19	0.46	-0.14	0	0	0
	-0.34	0.29	-0.13	0	0	0
	-0.01	0.43	0.33	0	0	0
	-0.36	0.16	0.20	0	-0.4	0
	-0.07	-0.15	-0.22	0	0	0
	0.03	0.21	0.05	0	0	0
	-0.02	0.04	0.01	0	0	0
	-0.38	-0.07	0.06	0	0	0
	-0.34	0.12	0.07	0	0	0
	0.29	0.21	-0.21	0.3	0	0
	0.12	-0.09	-0.31	0	0	0
	0.17	0.01	-0.30	0	0	0
	0.45	-0.20	-0.47	0	0	0
	0.35	-0.01	-0.18	0	0	0
	-0.01	0.05	0.10	0	0	0
	0.21	-0.18	-0.55	0	0	0
	0.20	-0.20	-0.12	0	0	0
	0.60	-0.26	0.07	0	0	0
	0.47	-0.08	0.19	0	0	0
	0.55	0.05	0.03	0	0	0
	0.31	0.00	0.17	0	0	0

Patient Number	Isocentre Position (mm)			Isocentre Shift (mm)		
	LR	AP	SI	LR	AP	SI
Patient 9	-0.08	-0.01	-0.22	0	0	0
	-0.14	-0.48	-0.30	0	0	0
	-0.08	-0.65	-0.33	0	0	0
	0.18	0.07	0.09	0	0	0
	-0.01	-0.10	-0.05	0	0	0
	-0.17	0.06	-0.01	0	0	0
	-0.38	-0.04	0.32	0	0	0
	-0.78	0.25	0.13	0	0	0
	-0.04	-0.03	-0.23	0	0	0
	-0.43	0.13	-0.15	0	0	0
	0.16	0.14	0.20	0	0	0
	-0.01	-0.11	-0.13	0	0	0
	-0.22	-0.09	0.05	0	0	0
	-0.06	0.11	-0.03	0	0	0
	-0.19	-0.08	-0.16	0	0	0
	-0.30	-0.05	-0.24	0	0	0
	0.04	0.05	-0.19	0	0	0
	-0.24	0.25	-0.17	0	0	0
	-0.30	0.13	-0.13	0	0	0
	-0.32	0.20	0.02	0	0	0
	-0.22	-0.34	0.14	0	0	0
	-0.10	-0.01	-0.10	0	0	0
	-0.06	0.45	-0.25	0	0	0
	-0.22	0.39	-0.13	0	0	0
	0.09	0.35	0.26	0	0	0
	-0.14	-0.26	0.07	0	-0.4	0
	-0.09	-0.69	0.00	0	0	0
	-0.08	-1.07	0.08	0	0	0
	-0.03	-0.84	0.13	0	0	0
	-0.26	-0.81	-0.10	0	0	0
Patient 10	0.41	0.22	0.52	0	0	0
	0.38	0.17	0.48	0	0	0
	-0.34	0.19	0.22	-0.4	0	-0.5
	0.09	0.26	-0.24	0	0	0
	-0.28	0.38	0.02	0	0	0
	-0.07	0.29	0.19	0	0	0
	-0.35	0.22	0.01	0	0	0
	-0.17	0.25	-0.03	0	0	0
	0.01	0.31	0.18	0	0	0
	0.11	0.04	-0.03	0	-0.3	0
	0.09	0.11	-0.38	0	0	0
	-0.19	0.20	-0.05	0	0	0
	0.02	-0.09	-0.41	0	0	0
	-0.01	0.12	-0.09	0	0	0.3
	-0.11	0.01	-0.10	0	0	0
	-0.10	0.13	0.21	0	0	0

Patient Number	Isocentre Position (mm)			Isocentre Shift (mm)		
	LR	AP	SI	LR	AP	SI
Patient 10	-0.17	-0.02	0.10	0	0	0
	-0.14	0.12	0.17	0	0	0
	-0.11	0.03	0.17	0	0	0
	-0.19	0.06	0.15	0	0	0
	0.10	-0.05	0.11	0	0	0
	0.06	-0.06	-0.01	0	0	0
	-0.24	0.03	0.44	0	0	0
	0.06	0.17	0.42	0	0	0
	-0.05	0.12	0.07	0	0	0
	-0.19	0.04	0.27	0	0	0
	-0.19	0.08	-0.05	0	0	0
	-0.09	0.08	0.46	0	0	0
	0.23	0.04	-0.06	0	0	0
	-0.16	0.07	0.31	0	0	0

Table 18: Raw set-up data for pilot study of 10 patients; Data is the corrected position of the isocentre and any shifts that were applied to that position

Patient Number	Isocentre Position (mm)			Isocentre Shift (mm)		
	LR	AP	SI	LR	AP	SI
Patient 1	-1.17	0.42	0.06	0	0	0
	0.01	-	0.08	0	0	0
	-0.26	0.33	0.16	0	0	0
	-0.35	0.25	-0.05	0	0	0
	-0.90	0.28	0.06	0	0	0
	-0.28	-	-0.06	0	0	0
	-	0.53	0.22	0	0	0
	-0.66	-	0.15	0	0	0
	-0.58	0.37	0.11	0	0	0
Patient 2	-	-0.28	0.05	0	0	0
	0.07	-	-0.07	0	0	0
	-0.13	-	0.18	0	0	0
	-0.05	0.05	-0.07	0	0	0
	0.35	-0.06	0.10	0	0	0
Patient 3	-0.27	0.09	0.05	0	0	0
	-0.28	0.24	0.18	0	0	0
	-0.37	-0.01	0.18	0	0	0
	-0.25	-0.07	0.41	0	0	0
	0.27	0.45	0.81	0	0	-0.4
	-0.18	-0.02	0.44	0	0	0
	0.00	0.11	-0.17	0	0	0
	-	0.09	0.20	0	0	0
	-0.42	-0.07	0.40	0	0	0
	0.27	-	0.89	0	0	0
	-0.20	-	0.23	0	0	0
	0.00	-	-0.20	0	0	0

Patient Number	Isocentre Position (mm)			Isocentre Shift (mm)		
	LR	AP	SI	LR	AP	SI
Patient 4	0.26	0.18	0.07	0	0	0
	-	0.49	0.35	0	0	0
	-0.14	-0.12	0.21	0	0	0
	-0.30	-0.07	0.26	0	0	0
	-0.04	-	0.06	0	0	0
	0.08	0.09	0.23	0	0	0
	0.26	0.22	0.15	0	0	0
	0.11	0.25	0.18	0	0	0
Patient 5	0.50	0.50	0.00	0	0	0
	-0.18	0.36	-0.31	0	0	0
	-0.01	-0.30	0.21	0	0	0
	-0.02	1.20	0.22	0	0	0
	0.23	0.24	0.08	0	0	0
	-0.16	0.23	0.23	0	0	0
Patient 6	0.01	0.01	-0.13	0	0	0
	0.01	0.44	-0.37	0	0	0
	-0.07	0.33	-0.03	0	0	0
	0.31	0.61	0.23	0	-0.4	0
	-0.27	0.24	0.12	0	0	0
	-0.01	0.26	0.16	0	0	0
	-0.04	0.07	0.15	0	0	0
Patient 7	0.32	0.16	0.39	0	0	0
	0.09	-0.10	0.23	0	0	0
	-0.01	0.06	0.05	0	0	0
	0.10	-	-0.18	0	0	0
	-	0.23	0.20	0	0	0
	-0.24	0.17	0.14	0	0	0
	0.18	0.34	0.15	0	0	0
	0.13	0.14	0.14	0	0	0
	-	0.22	0.34	0	0	0
	0.17	0.12	0.23	0	0	0
	0.28	0.05	0.36	0	0	0
	0.34	-	0.34	0	0	0
Patient 8	-0.02	-0.38	-0.11	0	0	0
	-0.03	-0.39	0.35	0	0.4	0
	0.08	0.08	-0.02	0	0	0
	0.24	0.19	0.28	0	0	0
	-0.26	0.13	-0.16	0	0	0
	-0.01	0.01	0.10	0	0	0
	-	0.40	0.49	0	0	0
	-0.29	-	0.27	0	0	0
	-0.13	-	0.34	0	0	0
	-0.05	0.10	0.26	0	0	0
	-0.24	-0.15	0.16	0	0	0
Patient 9	-0.41	0.04	0.31	0	0	0
	-0.27	0.27	0.68	0	0	-0.5
	-0.31	0.40	-0.01	0	0	0

Patient Number	Isocentre Position (mm)			Isocentre Shift (mm)		
	LR	AP	SI	LR	AP	SI
Patient 9	-0.46	0.19	-0.02	0.3	0	0
	-0.16	-0.02	-0.07	0	0	0
	-0.32	0.10	-1.06	0	0	0
	-0.11	0.43	-0.39	0	0	-0.4
	-0.08	0.53	-0.64	0	0	0
	0.00	-	0.17	0	0	0
	-	0.14	-0.30	0	0	0
	-0.02	0.50	0.05	0	0	0
	-	0.20	0.07	0	0	0
	0.07	0.13	-0.18	0	0	0
Patient 10	-0.01	-0.23	-0.04	0	0	0
	0.14	-0.15	0.05	0	0	0
	-	0.04	-	0	0	0
	0.16	-0.19	0.09	0	0	0
	0.24	-0.15	-0.19	0	0	0
	0.30	-0.05	-0.19	0	0	0
	0.08	-0.22	0.01	0	0	0
	-0.20	-0.05	-0.29	0	0	0
	0.34	-	-0.19	0	0	0
Patient 11	0.14	0.28	0.20	0	0	0
	-0.22	-	0.19	0	0	0
	-0.26	-0.01	0.08	0	0	0
	0.12	0.29	0.01	0	0	0
	-0.15	0.43	0.30	0	0	0
	-1.19	-	0.12	0	0	0
	-0.03	0.04	0.19	0	0	0
	-0.24	0.43	0.06	0	0	0
	0.17	-0.28	0.03	0	0	0
	0.05	-0.19	-0.31	0	0	0
Patient 12	0.67	0.66	0.02	-0.6	0	0
	0.64	0.29	0.38	0	0	0
	0.22	0.27	0.32	0	0	0
	-	0.39	0.22	0	-0.3	0
	-0.35	-0.11	0.15	0	0	0
	-0.52	-0.22	0.50	0	0	0
	-0.38	0.11	0.17	0	0	0
	0.05	-	0.09	0	0	0
	-	-0.03	-0.11	0	0	0
	0.26	0.03	0.09	0	0	0
Patient 13	0.41	-0.04	0.13	-0.4	0	0
	-0.27	0.01	0.02	0	0	0
	-0.29	0.00	0.38	0.3	0	0
	-	0.10	0.27	0	0	0
	0.22	0.29	0.26	0	0	0
	0.23	-0.02	0.10	0	0	0

Patient Number	Isocentre Position (mm)			Isocentre Shift (mm)		
	LR	AP	SI	LR	AP	SI
Patient 14	0.18	0.41	0.08	0	0	0
	-0.13	0.37	0.26	0	-0.4	0
	-0.24	-0.04	0.10	0	0	0
	0.09	-0.04	0.09	0	0	0
	0.00	0.20	-0.05	0	0	0
Patient 15	-0.12	-0.08	-0.18	0	0	0
	-0.27	0.12	-0.01	0	0	0
	-0.36	0.49	-0.33	0	0	0
	-0.18	-0.13	-0.20	0	0	0
	0.00	-0.03	-0.06	0	0	0
	0.11	0.04	-0.18	0	0	0
	-0.19	0.08	0.04	0	0	0
	0.34	-0.02	-0.34	0	0	0
	-0.17	-0.05	-0.01	0	0	0
Patient 16	-0.14	-0.23	0.40	0	0	0
	0.04	0.08	0.46	0	0	-0.3
	0.21	-0.14	-0.25	0	0	0
	-	0.23	-0.16	0	0	0
	-0.09	0.06	0.20	0	0	0
	-0.19	-0.12	0.07	0	0	0
	-0.12	0.25	0.19	0	0	0
	0.09	-0.10	-0.21	0	0	0
	-	0.06	0.26	0	0	0
	0.14	0.16	-0.12	0	0	0
Patient 17	-0.02	-0.34	0.10	0	0	0
	0.20	-0.25	0.26	0	0	0
	0.20	0.27	-0.07	0	0	0
	0.24	-0.10	-0.04	0	0	0
	0.21	-0.24	0.25	0	0	0
	0.32	-0.29	-0.16	-0.2	0	0
	0.30	-0.04	-0.01	0	0.2	0
	0.02	0.27	-0.05	0	0	0
	0.08	0.36	0.07	0	0	0
	-	0.02	0.02	0	0	0
	-	-0.15	0.15	0	0	0
Patient 18	0.24	0.11	-0.06	0	0	0
	0.09	-	0.19	0	0	0
	0.06	0.20	-0.26	0	0	0
	0.28	0.13	0.15	0	0	0
	0.26	0.02	-0.10	0	0	0
	-0.03	0.18	0.37	0	0	0
	0.29	-	0.02	0	0	0
	0.15	-0.04	0.41	0	0	0
	0.16	-0.11	0.02	0	0	0
	0.28	0.05	0.24	0	0	0
	0.16	-0.13	0.09	0	0	0

Patient Number	Isocentre Position (mm)			Isocentre Shift (mm)		
	LR	AP	SI	LR	AP	SI
Patient 19	0.28	-0.70	0.39	0	0.7	0
	0.43	-0.03	0.30	0	0	-0.3
	-0.63	-	-0.20	-0.3	0	0
	0.00	0.33	-0.13	0	0	0
	-	-0.16	-0.48	0	0	0
	-0.15	0.37	-0.02	0	0	0
Patient 20	0.27	0.03	0.35	0	0	0.3
	-0.04	0.21	-0.03	0	0	0
	0.18	0.12	-0.11	0	0	0
	0.67	0.21	-0.15	0	0	0
	0.70	0.30	-0.09	-0.5	-0.2	0
	-0.03	-	0.00	0	0	0
	0.16	0.27	-0.02	0	0	0
Patient 21	-0.16	0.11	0.21	0	0	0
	0.14	0.16	-0.27	0	0	0
	0.08	0.03	-0.07	0	0	0
	-0.02	0.20	-0.07	0	0	0
	0.15	0.13	-0.02	0	0	0
	0.21	0.02	-0.39	0	0	0
	-0.02	-0.11	-0.23	0	0	0
Patient 22	-0.33	0.33	0.16	0	0	0
	-0.01	0.41	0.28	0	-0.3	0
	0.19	-0.29	0.06	0	0	0
	-0.14	-0.30	0.12	0	0	0
	-0.14	-0.10	0.17	0	0	0
	-0.09	0.01	0.11	0	0	0
	-0.28	-0.08	0.22	0	0	0
	0.29	-0.43	0.29	0	0	0
	-0.20	-0.19	0.15	0	0	0
	0.18	-0.30	0.36	0	0	0
	0.02	-0.14	0.33	0	0	-0.3
Patient 23	0.08	0.52	0.29	0	0	0
	0.30	0.96	-0.03	0	-0.5	0
	0.13	0.18	0.03	0	0	0
	0.16	0.16	0.39	0	0	0
	-0.02	-0.22	0.17	0	0	0
	0.36	-0.38	0.40	0	0	0
	0.29	0.09	0.23	-0.2	0	0
	0.18	-0.15	-0.11	0	0	-0.2
	0.60	-0.36	-0.26	0	0	0
	-0.22	0.00	-0.05	0	0	0
	0.22	0.29	0.21	0	0	0
	0.06	0.22	-0.19	0	0	0
	-0.07	-0.12	-0.11	0	0	0
	-0.03	-0.14	-0.37	0	0	0
	-0.06	-0.34	-0.02	0	0	0

Patient Number	Isocentre Position (mm)			Isocentre Shift (mm)		
	LR	AP	SI	LR	AP	SI
Patient 24	-0.40	0.57	-0.02	0	0	0
	-0.52	0.66	-0.83	0.4	-0.6	0
	-0.10	-0.08	-0.59	0	0	0.5
	-0.01	-0.28	0.02	0	0	0
	-0.37	0.11	0.22	0	0	0
	-0.11	0.22	0.28	0	0	0
	0.06	-	0.03	0	0	0
	-	0.22	0.35	0	0	0
	-0.12	0.22	0.04	0	0	0
	-0.11	-	-0.26	0	0	0
	-0.35	-0.13	0.46	0	0	0
	-0.19	0.01	0.10	0	0	0
	-0.28	-0.28	-0.14	0	0	0
Patient 25	-	0.06	0.23	0	0	0
	-0.16	0.03	0.03	0	0	0
	-0.22	-0.01	0.03	0	0	0
	-0.04	0.06	0.01	0	0	0
	-0.18	0.09	0.35	0	0	0
	-0.05	-0.05	0.31	0	0	0
	0.09	-0.18	0.15	0	0	0
	-0.22	-0.06	-0.22	0	0	0
	-0.24	0.03	0.03	0	0	0
	-0.01	0.00	0.27	0	0	0
Patient 26	0.15	-0.56	0.31	0	0	0
	0.43	-0.03	0.19	0	0	0
	0.12	-	0.43	0	0	0
	-0.36	-0.55	0.19	0	0	0
	-0.07	-0.31	-0.08	0	0.3	0
	0.05	-0.01	0.32	0	0	0
	-0.37	-0.06	0.21	0	0	0
	-0.53	0.12	0.04	0.4	0	0
	-0.10	0.07	0.05	0	0	0
Patient 27	0.04	-0.18	-0.05	0	0	0
	-0.27	-0.13	0.24	0	0	0
	-0.34	-0.22	-0.06	0	0	0
	-0.13	0.18	0.24	0	0	0
	-0.08	0.21	-0.01	0	0	0
	-0.80	-0.63	0.31	0	0	0
	-	-0.72	0.12	0	0.6	0
	-0.08	-	-0.13	0	0	0
	-0.27	-0.13	0.15	0	0	0
	-0.02	0.13	0.06	0	0	0
Patient 28	0.02	-	0.05	0	0	0
	-	0.31	0.25	0	0	0
	0.52	0.17	0.01	0	0	0
	0.13	0.27	0.20	0	0	0
	0.33	0.49	0.25	0	0	0

Patient Number	Isocentre Position (mm)			Isocentre Shift (mm)		
	LR	AP	SI	LR	AP	SI
Patient 28	0.20	0.18	0.24	0	0	0
	0.10	0.26	0.29	0	0	0
	0.33	0.25	0.05	0	0	0
	0.36	0.25	0.05	-0.3	0	0
	0.00	0.29	0.21	0	0	0
Patient 29	0.36	0.24	0.48	0	0	0
	-0.16	0.08	0.57	0	0	-0.4
	0.30	0.21	0.04	0	0	0
	0.25	0.10	-0.08	0	0	0
	-0.06	0.04	-0.08	0	0	0
	0.17	-0.01	-0.36	0	0	0
	-0.14	0.21	-0.12	0	0	0
	0.00	0.02	0.07	0	0	0
Patient 30	0.15	-0.01	0.23	0	0	0
	0.25	0.21	0.28	0	0	0
	0.02	0.23	-0.04	0	0	0
	0.26	0.56	0.17	0	0.2	0
	0.03	0.38	0.04	0	0.3	0
	0.04	0.72	0.01	0	-0.5	0
	0.00	-0.11	0.14	0	0	0
	0.26	0.02	-0.04	0	0	0
Patient 31	-0.07	0.39	0.25	0	0	0
	-0.23	0.06	0.40	0	0	0
	-0.18	0.27	0.22	0	0	0
	0.15	-0.10	0.06	0	0	0
	-0.15	-0.18	0.14	0	0	0
	-0.06	0.23	0.22	0	0	0
	-0.17	0.03	0.25	0	0	-0.2
	-0.14	0.03	-0.04	0	0	0
	-0.12	0.18	0.08	0	0	0
	-0.15	0.13	-0.12	0	0	0
Patient 32	0.35	0.05	0.12	0	0	0
	0.13	0.25	0.18	0	0	0
	0.12	0.23	0.34	0	0	0
	0.41	-0.01	-0.03	0	0	0
	0.29	0.21	0.19	0	0	0
	0.56	0.14	0.05	0	0	0
	0.42	-	0.29	-0.4	0	0
	-0.15	0.11	0.29	0	0	-0.2
	-0.12	0.23	0.39	0	0	-0.2
	0.03	0.25	0.20	0	0	0
	-	0.00	-0.04	0	0	0
	0.04	-0.02	-0.08	0	0	0
	-	-0.20	-0.30	0	0	0
	-0.31	0.01	0.01	0	0	0
	0.79	0.10	0.17	0	0	0

Patient Number	Isocentre Position (mm)			Isocentre Shift (mm)		
	LR	AP	SI	LR	AP	SI
Patient 33	0.79	0.10	0.17	0	0	0
	0.42	0.25	-0.07	0	0	0
	0.34	0.16	-0.22	0	0	0
	0.41	0.36	-0.10	-0.3	0	0
	0.03	0.13	-0.12	0	0	0
	-	0.12	0.03	0	0	0
	0.27	-	-0.19	0	0	0
	0.25	0.23	0.01	0	0	0
Patient 34	-	0.08	0.34	0	0	0
	0.06	0.24	0.11	0	0	0
	0.15	0.15	0.06	0	0	0
	-0.14	0.25	0.19	0	0	0
	0.20	0.25	0.37	0	0	0
	0.23	0.09	0.21	0	0	0
	0.24	0.28	0.12	0.2	0	0
	0.34	0.14	0.11	-0.3	0	0
	0.07	0.05	0.48	0	0	0
	0.50	0.31	0.27	0	0	-0.3
	0.07	0.04	0.14	0	0	0
	-0.04	0.24	-0.25	0	0	0
Patient 35	0.05	0.12	0.04	0	0	0
	0.18	0.18	0.12	0	0	0
	-0.05	0.09	0.06	0	0	0
	0.08	0.23	0.07	0	0	0
	-0.07	0.42	-0.40	0	0	0
	0.17	0.27	0.42	0	0	0
	0.18	0.00	0.13	0	0	0
	0.27	0.30	0.14	-0.3	0	0
	-0.32	-	0.60	0	0.2	0
	-	-0.14	0.11	0	0	-0.3
	-0.27	0.11	0.15	0	0	0
	0.18	-0.13	-0.12	0	0	0
	-0.11	0.24	0.04	0	0	0
Patient 36	0.22	0.28	-0.10	0	0	0
	-0.15	0.21	0.07	0	0	0
	0.37	0.28	-0.11	0	0.2	0
	0.08	0.18	-0.18	0	0	0
	-0.06	0.23	0.27	0	0	0
	0.18	0.07	0.26	0	0	0
	0.04	0.19	-0.06	0	0	0
	-0.08	0.09	0.29	0	0	0
	-0.05	0.27	-0.21	0	0	0
	0.01	0.00	-0.03	0	0	0
	0.09	-0.14	-0.25	0	0	0
Patient 37	0.14	0.31	0.18	0	0	0
	0.30	0.02	0.30	0	0	0
	0.17	0.00	0.11	0	0	0

Patient Number	Isocentre Position (mm)			Isocentre Shift (mm)		
	LR	AP	SI	LR	AP	SI
Patient 37	-0.17	0.08	-0.10	0	0	0
	0.30	0.00	-0.11	0	0	0
	0.31	0.24	-0.50	0	0	0
	0.28	-0.20	-0.01	0	0	0
	0.19	0.10	0.03	0	0	0
Patient 38	0.25	0.29	0.09	0	0	0
	0.01	0.03	0.06	0	0	0
	0.06	0.40	-0.07	0	0	0
	0.12	0.17	0.05	0	0	0
	0.03	0.16	0.18	0	0	0
	-0.05	0.12	-0.21	0	0	0
	-0.01	0.11	-0.06	0	0	0
	0.04	-	-0.03	0	0	0
	0.01	-0.06	0.22	0	0	0
	0.03	-0.01	0.01	0	0	0
	0.10	-	-0.16	0	0	0
	-	0.16	0.09	0	0	0
Patient 39	0.20	-0.25	-0.40	0	0	0
	0.36	-0.06	-0.16	0	0	0
	0.71	-0.23	-0.32	0	0	0.3
	0.50	-0.22	0.33	-0.4	0	0
	0.16	-0.07	0.41	0	0	0
	0.16	0.14	-0.03	0	0	0
	0.21	0.08	0.04	0	0	0
	0.09	-0.18	-0.24	0	0	0
	0.01	-0.04	-0.31	0	0	0
Patient 40	-0.10	0.35	-0.04	0	0	0
	0.13	-0.15	0.01	0	0	0
	-0.14	0.09	0.06	0	0	0
	0.04	0.17	-0.06	0	0	0
	0.18	0.01	-0.08	0	0	0
	-	0.08	-0.07	0	0	0
	-0.04	-	0.14	0	0	0
	-0.03	0.22	0.00	0	0	0
	-0.01	0.21	-0.02	0	0	0
	-	-0.04	0.01	0	0	0
	-0.26	0.25	-0.05	0	0	0
	0.28	-0.35	-0.13	0	0	0
Patient 41	-0.20	-0.40	-	0	0	0
	0.04	0.00	0.01	0	0	0
	-0.15	-0.35	-0.02	0	0	0
	-0.27	-0.37	-0.04	0	0	0
	-0.35	-0.22	0.11	0.3	0	0
	-0.32	0.10	0.01	0	0.2	0
	-0.02	0.04	0.07	0	0	0
	-0.13	-0.02	-0.07	0	0	0

Patient Number	Isocentre Position (mm)			Isocentre Shift (mm)		
	LR	AP	SI	LR	AP	SI
Patient 41	0.33	-0.45	-0.18	0	0	0
	-0.12	-	-0.10	0	0	0
	-0.12	-0.28	-0.12	0	0	0
	0.06	-0.08	-0.13	0	0	0
Patient 42	0.09	-0.64	0.22	0	0	0
	-0.22	-0.25	0.22	0	0	0
	0.28	-0.50	0.38	0	0	-0.3
	0.05	-	0.34	0	0	0
	0.18	-0.44	0.23	0	0.3	0
	0.12	-0.39	0.28	0	0	-0.2
	0.04	-0.26	0.37	0	0	0
	0.05	-0.33	-0.09	0	0	0
	0.07	-0.60	-0.06	0	0	0
Patient 43	0.18	-0.18	0.15	0	0	0
	0.48	0.02	0.23	0	0	0
	0.45	0.09	0.13	-0.3	0	0
	0.11	0.36	0.23	0	0	0
	-0.49	0.35	0.37	0	0	-0.3
	0.20	-	-0.16	0	-0.3	0
	-0.34	0.03	0.09	0	0	0
	0.29	0.07	-0.09	0	0	0
	0.07	-0.37	-0.12	0	0	0
	-0.02	-0.20	-0.04	0	0	0
	0.03	-0.25	0.15	0	0	0
Patient 44	-0.05	-0.24	-0.02	0	0	0
	0.00	0.23	-0.04	0	0	0
	0.10	0.09	-0.06	0	0	0
	0.09	0.12	-0.12	0	0	0
	-0.16	0.42	-0.46	0	0	0
	0.09	0.26	-0.08	0	0	0
	0.00	0.01	-0.04	0	0	0
	-0.12	0.18	-0.19	0	0	0
	0.01	0.25	-0.17	0	0	0
	-0.22	0.13	-0.02	0	0	0
	-0.01	0.18	-0.09	0	0	0
Patient 45	-0.32	-0.05	-0.01	0	0	0
	0.06	-0.20	-0.08	0	0	0
	-0.02	-0.26	-0.11	0	0	0
	-0.26	-0.20	-0.06	0	0	0
	-0.38	-0.14	-0.24	0	0	0
	0.05	-	-0.19	0	0	0
	-0.13	-0.12	-0.09	0	0	0
	-0.30	-0.14	-0.05	0	0	0
	-0.54	-0.08	-0.10	0	0	0
	-0.45	0.18	-0.09	0.3	0	0
	-0.18	-0.19	-0.23	0	0	0

Patient Number	Isocentre Position (mm)			Isocentre Shift (mm)		
	LR	AP	SI	LR	AP	SI
Patient 45	-0.16	0.17	-0.11	0	0	0
	0.03	0.12	-0.14	0	0	0
Patient 46	-0.38	0.37	0.46	0	0	0
	0.54	0.37	-0.27	0	-0.4	0
	0.05	0.13	-0.03	0	0	0
	0.06	0.20	-0.08	0	0	0
	0.14	0.25	0.10	0	0	0
	-0.04	0.34	-0.18	0	0	0
	0.39	-0.18	-0.04	0	0	0
	-0.08	-0.05	-0.04	0	0	0
	-0.49	0.22	-0.18	0	0	0
	-0.08	-0.04	-0.07	0	0	0
	0.27	0.23	-0.19	0	0	0
	0.08	0.02	-0.10	0	0	0
Patient 47	-0.35	-	0.05	0	0	0
	-0.16	0.13	-0.19	0	0	0
	-0.08	0.26	0.03	0	0	0
	-0.06	0.54	-0.09	0	0	0
	-0.71	0.31	-0.28	0	0	0
	-0.07	0.12	-0.01	0	0	0
	-0.25	0.30	-0.13	0	0	0
	-	0.24	-0.19	0	0	0
	-0.16	0.20	0.06	0	0	0
	-0.33	0.29	-0.16	0	-0.3	0
	-0.06	0.41	-0.14	0	0	0
	-0.55	-0.06	-0.16	0	0	0
	0.09	0.35	0.07	0	0	0
	-0.20	0.24	-0.19	0	0	0
	-0.33	-	-0.02	0	0	0
	-0.16	0.25	-0.14	0	0	0
Patient 48	-0.60	0.11	0.01	0	0	0
	-0.07	-0.28	-0.12	0	0	0
	-0.19	-0.27	0.13	0	0	0
	-0.21	0.07	0.10	0	0	0
	0.01	0.44	0.13	0	0	0
	-0.06	-0.20	-0.18	0	0	0
	-0.17	0.09	-0.03	0	0	0
	-0.37	0.03	-0.04	0	0	0
	-0.51	-0.05	-0.12	0	0	0
	-0.42	0.09	-0.23	0.4	0	0
	0.01	-0.08	0.17	0	0	0
	-0.09	0.07	-0.33	0	0	0
	-	-0.23	-0.31	0	0	0.3
	0.00	0.09	-0.10	0	0	0
	0.20	-0.10	-0.39	0	0	0

Patient Number	Isocentre Position (mm)			Isocentre Shift (mm)		
	LR	AP	SI	LR	AP	SI
Patient 49	-0.73	-0.72	-0.06	0	0	0
	-0.18	0.14	-0.21	0	0.5	0
	-0.94	0.16	-0.13	0	0	0
	-0.05	-0.06	-0.16	0	0	0
	-0.36	-0.30	0.09	0	0	0
	-0.03	-0.20	-0.03	0	0	0
	-0.22	0.25	0.13	0	0	0
	-0.29	0.04	0.19	0	0	0
	0.31	0.37	0.13	0	0	0
	-0.18	0.22	-0.17	0	0	0
	0.02	-	0.01	0	0	0
	-	0.29	0.00	0	0	0
Patient 50	-0.16	0.41	0.11	0	0	0
	0.04	0.07	0.16	0	-0.4	0
	0.01	0.01	0.20	0	0	0
	0.09	-0.05	0.10	0	0	0
	-0.07	0.45	0.58	0	0	0
	-0.03	0.04	0.27	0	0	0
	-0.18	0.03	0.32	0	0	-0.3
	-0.06	-0.05	-0.16	0	0	0
	-0.29	0.15	-0.14	0	0	0
Patient 51	0.14	0.10	0.06	0	0	0
	0.00	-0.10	0.21	0	0	0
	0.04	-0.04	-0.05	0	0	0
	-0.94	-0.09	0.04	0	0	0
	-0.01	-0.12	0.07	0	0	0
	-0.25	-	0.11	0	0	0
	-0.09	-0.10	0.03	0	0	0
	-0.45	-0.17	0.15	0	0	0
	-0.17	-0.17	0.10	0	0	0
	-0.02	0.25	-0.07	0	0	0
	0.16	-0.05	-0.20	0	0	0
	-0.04	-0.34	0.15	0	0	0
Patient 52	0.32	-0.16	0.25	0	0	0
	0.26	-0.09	0.22	0	0	0
	-0.04	0.11	-0.22	0	0	0
	0.29	-0.14	-0.09	0	0	0
	0.65	-0.09	-0.38	0	0	0
	0.43	0.08	-0.06	-0.3	0	0
	0.05	0.05	-0.19	0	0	0.2
	-0.02	-0.13	0.11	0	0	0
	-0.10	-0.20	-0.11	0	0	0
	0.04	-0.01	0.31	0	0	0
	-0.24	0.09	0.37	0	0	0
	0.00	-0.19	-0.34	0	0	0
	-0.12	-	-0.30	0	0	0
	0.01	-0.15	0.14	0	0	0

Patient Number	Isocentre Position (mm)			Isocentre Shift (mm)		
	LR	AP	SI	LR	AP	SI
Patient 53	-0.35	0.01	0.03	0	0	0
	0.27	-0.08	-0.02	0	0	0
	0.23	-0.14	-0.02	0	0	0
	0.03	-0.24	-0.04	0	0	0
	0.12	-0.09	0.03	0	0	0
	0.09	0.11	-0.12	0	0	0
	0.20	0.19	-0.07	0	0	0
	0.14	0.36	0.01	0	0	0
Patient 54	0.39	-0.46	-0.29	0	0	0
	0.15	0.10	-0.03	0	0	0
	0.08	-0.24	0.07	0	0	0
	-0.30	-	-0.01	0	0	0
	-0.12	0.12	-0.02	0	0	0
	-	0.18	0.03	0	0	0
	-	-0.08	0.28	0	0	0
	-0.01	-	0.05	0	0	0
	-0.11	0.24	0.11	0	0	0
	0.33	-0.16	0.32	0	0	0
	0.23	0.17	0.22	0	0	0
Patient 55	-0.68	0.10	0.27	0	0	0
	0.17	0.52	0.27	0	0	0
	-0.16	0.52	0.27	0	-0.4	0
	-0.10	0.07	-0.13	0	0	-0.2
	-0.24	0.41	0.04	0	0	0
	-0.13	0.13	-0.25	0	0	0
	-0.21	0.13	-0.16	0	0	0
	-0.10	0.08	0.03	0	0	0
	-0.25	0.34	0.21	0	0	0
	-0.13	0.16	0.04	0	0	0
	-0.47	-0.55	-0.23	0	0	0
	-0.23	-0.11	0.00	0	0	0
Patient 56	0.00	-	0.10	0	0	0
	-0.15	0.56	0.37	0	-0.5	0
	-0.32	0.50	0.41	0	0	-0.3
	-0.13	0.18	0.11	0	0	0
	-0.17	0.00	0.07	0	0	0
	-0.09	0.22	0.07	0	0	0
	0.04	0.27	-0.02	0	0	0
	0.00	0.07	-0.15	0	0	0
	0.13	-0.09	0.13	0	0	0
	-0.25	-0.07	0.03	0	0	0
Patient 57	0.13	-	-0.08	0	0	0
	-0.08	-0.03	0.12	0	0	0
	-0.03	-0.09	0.03	0	0	0
	-0.10	-0.05	-0.02	0	0	0
	-0.31	0.23	-0.03	0	0	0

Patient Number	Isocentre Position (mm)			Isocentre Shift (mm)		
	LR	AP	SI	LR	AP	SI
Patient 57	-0.38	-0.16	0.09	0.3	0	0
	0.15	-0.13	-0.02	0	0	0
	-0.28	0.29	0.03	0	0	0
	0.32	0.08	0.19	0	0	0
	0.21	-0.04	-0.01	0	0	0
Patient 58	0.58	-0.42	-0.26	0	0	0
	-0.16	0.02	0.07	-0.5	0	0
	-0.16	0.18	0.04	0	0	0
	-0.45	-0.28	-1.36	0	0	0
	0.05	-0.06	-0.06	0	0	0
	0.32	-0.09	0.18	0	0	0
	0.06	0.17	0.00	0	0	0
	-0.06	-0.26	0.25	0	0	0
Patient 59	0.31	0.24	0.18	0	0	0
	0.58	0.01	-0.03	-0.3	0	0
	-0.18	0.09	-0.18	0	0	0
	-0.28	-0.14	0.13	0	0	0
	-0.13	-0.10	0.09	0	0	0
	-0.20	0.09	0.03	0	0	0
	-0.17	0.08	-0.10	0	0	0
	-0.06	0.27	-0.03	0	0	0
	-0.21	0.27	0.09	0	0	0
	-0.08	0.17	-0.03	0	0	0
Patient 60	-0.76	0.08	-0.05	0	0	0
	-0.23	-0.19	-0.05	0	0	0
	-0.15	-0.19	0.05	0	0	0
	-0.15	-0.07	-0.67	0	0	0
	-0.16	-0.20	0.04	0	0	0
	-0.21	0.06	0.21	0	0	0
	-0.26	0.07	0.09	0	0	0
	-0.90	-0.40	-0.03	0	0	0
	-0.03	-0.09	0.54	0	0	0
	-0.33	-0.25	0.14	0	0	0
	-0.33	-0.30	0.38	0	0.3	0
	-0.28	-0.33	0.16	0.3	0	0
	-0.05	0.11	0.13	0	0	0
	-0.21	0.13	0.23	0	0	0
Patient 61	0.03	0.21	0.18	0	0	0
	-0.10	0.36	0.07	0	-0.2	0
	0.02	0.33	0.16	0	0	0
	0.24	0.19	-0.06	0	0	0
	0.02	0.36	0.11	0	0	0
	0.03	0.22	-0.03	0	0	0
	0.18	0.23	0.24	0	0	0
	0.09	-	0.21	0	0	0
	-	0.19	-0.01	0	0	0

Patient Number	Isocentre Position (mm)			Isocentre Shift (mm)		
	LR	AP	SI	LR	AP	SI
Patient 61	0.23	0.17	0.18	0	0	0
	-0.01	0.27	0.08	0	0	0
	0.21	0.10	0.22	0	0	0
Patient 62	0.29	0.28	0.32	0	0	0
	0.02	-0.30	-0.27	0	0	0
	0.27	0.06	0.30	0	0	0
	0.37	0.27	-0.10	0	0	0
	0.22	-0.03	-0.02	0	0	0
	0.07	-0.06	0.17	0	0	0
	0.34	0.17	0.07	0	0	0
	0.15	0.21	0.06	0	0	0
	0.12	0.40	0.32	0	0	0
	0.04	0.05	0.19	0	0	0
	-	0.16	0.28	0	0	0
	-0.05	-0.14	0.08	0	0	0

Table 19: Raw set-up data for study of 62 patients. Data is the corrected position of the isocentre and any shifts that were applied to that position

7.5 Raw Organ Motion Centroid Shifts

Patient Identifier	Prostate Centroid Shift (mm)			Rectum Centroid Shift (mm)		
	LR	AP	SI	LR	AP	SI
P1	-2.0	-2.6	-4.2	-0.2	-2.4	-8.6
P2	-0.6	-2.0	-4.6	-3.9	-0.4	0.9
P3	-0.1	-0.1	1.6	0.0	-0.5	-5.4
P4	-0.6	-6.7	-5.7	0.4	-3.1	-11.3
P5	0.7	-1.6	-3.9	-1.8	-1.1	10.9
P6	0.4	3.6	1.5	0.3	0.1	4.9
P7	-1.6	-2.5	-2.1	-1.9	3.5	5.2
P8	0.8	-4.3	-11.9	-0.1	-6.5	-10.0
P9	1.7	1.8	2.8	-0.3	5.2	7.3

Table 20: Raw centroid shifts determined in organ motion study

7.6 Raw Target Delineation Study Centroid Data

Patient Identifier	Prostate Centroid Position (cm)			Rectum Centroid Position (cm)		
	LR	AP	SI	LR	AP	SI
P1a	0.19	-0.95	-0.70	0.18	-4.36	-1.40
P1a	0.26	-1.15	-1.15	0.15	-4.42	-1.33
P1a	0.31	-0.97	-1.13	0.13	-4.41	-1.17
P1b	0.26	-1.11	-1.09	0.00	-4.47	-0.31
P1b	0.21	-1.08	-0.91	-0.06	-4.58	0.30
P1b	0.31	-1.06	-1.17	0.01	-4.50	0.10
P2a	0.20	-1.32	-15.49	0.06	-5.04	15.50
P2a	0.23	-1.31	-15.49	0.07	-5.23	15.28
P2a	0.22	-1.20	-15.43	-0.02	-5.38	14.67
P2b	0.24	-0.96	-15.34	0.09	-5.05	15.01
P2b	0.19	-0.90	-15.67	0.01	-5.47	13.97
P2b	0.22	-0.89	-15.51	0.06	-5.33	14.37
P3a	0.08	0.87	-15.28	-0.23	-3.36	-15.34
P3a	0.07	1.07	-15.28	-0.25	-3.37	-15.40
P3a	0.08	0.64	-15.17	-0.26	-3.52	-15.16
P3b	-0.08	0.62	-15.50	-0.42	-3.01	-15.86
P3b	-0.13	0.80	-15.80	-0.43	-3.06	-16.01
P3b	-0.16	0.80	-15.83	-0.44	-3.09	-15.81
P4a	-0.11	0.30	0.68	-0.16	-3.06	1.60
P4a	-0.06	0.58	1.13	-0.25	-3.26	1.49
P4a	-0.06	0.66	0.88	-0.27	-3.25	1.14
P4b	-0.03	-0.13	1.87	-0.17	-3.72	2.60
P4b	-0.07	-0.26	1.90	-0.29	-3.90	2.18
P4b	-0.05	-0.38	2.03	-0.20	-3.44	2.66
P5a	-0.03	-2.53	-24.32	0.35	-6.42	24.34
P5a	0.03	-2.58	-24.35	0.36	-6.37	24.58
P5a	0.05	-2.63	-24.28	0.38	-6.32	24.63
P5b	0.13	-2.35	-24.05	0.32	-6.94	23.61
P5b	0.13	-2.52	-23.88	0.30	-7.08	23.40
P5b	0.07	-2.40	-24.02	0.32	-6.90	23.67
P6a	-0.54	0.20	-16.21	-0.84	0.20	-14.90
P6a	-0.64	0.15	-16.20	-0.84	0.15	-15.06
P6a	-0.61	0.19	-16.28	-0.91	0.19	-15.34
P6b	-0.60	-0.47	-16.78	-0.79	-0.47	-16.04
P6b	-0.66	-0.39	-16.60	-0.74	-0.39	-15.67
P6b	-0.61	-0.56	-16.39	-0.64	-0.56	-15.89

Table 21: Individual centroids positions determined in the target delineation study

8 References

Aaltonen P, Brahme A, Lax I, Levernes S, Naslund I, Reitan JB and Turesson I, Specification of dose delivery in radiation therapy: Recommendation by the Nodric Association of Clinical Physics (NACP). Acta Oncologica 1997, 36 (Supplement 10), 1-32.

Althof VGM, Hoekstra CJM, and Te Loo HJ, Variation in prostate position relative to adjacent bony anatomy. International Journal of Radiation Oncology, Biology, Physics 1996, 34(3), 709-715.

Antolak JA, Rosen II, Childress CH, Zagars GK and Pollack A, Prostate target volume variations during a course of radiotherapy. International Journal of Radiation Oncology, Biology, Physics 1998, 42(3), 661-672.

Australian Bureau of Statistics, Cancer trends, in Year Book Australia at http://www.abs.gov.au/Ausstats/abs@.nsf/0/518663B20E8B062CCA256F720083301C?Open last cited 16/08/2005.

Balter JM, Sandler HM, Lam K, Bree RL, Lichter AS and Ten Haken RK, Measurement of prostate movement over the course of routine radiotherapy using implanted markers. International Journal of Radiation Oncology, Biology, Physics 1995, 31(1), 113-118.

Baxter BS, Hitchner LE and Maguire GQ. AAPM Report No. 10: A Standard Format for Digital Image Exchange. American Institute of Physics, New York, NY, 1982.

Bel A, van Herk M, Bartelink H, Lebesque J, A verification procedure to improve patient setup accuracy using portal images. Radiotherapy and Oncology 1993, 29, 253-260.

Bel A, Vos PH, Rodrigus PTR, Creutzberg CL, Visser AG, Stroom JC and Lebesque JV, High-precision prostate cancer irradiation by clinical application of an offline patient setup verification procedure, using portal imaging. International Journal of Radiation Oncology, Biology, Physics 1996, 35(2), 321-332.

Bel A, van Herk M, Lebesque JV, Target margins for random geometrical treatment uncertainties in conformal radiotherapy. Medical Physics 1996, 23: 1537-1545.

Booth JT and Zavgorodni SF, Set-up error & organ motion uncertainty: A Review. Australasian Physical & Engineering Sciences in Medicine 1999, 22(2), 29-47.

Bosch W. Specifications for Tape/Network Format for Exchange of Treatment Planning Information, Version 4.00. Image Guided therapy Center at Washington University, http://rtog3dqa.wustl.edu, 1999.

Chung PWM, Haycocks T, Brown T, Cambridge Z, Kelly V, Alasti H, Jaffray DA and Catton CN, On-line aSi portal imaging of implanted fiducial markers for the reduction of interfraction error during conformal radiotherapy of prostate carcinoma. International Journal of Radiation Oncology, Biology, Physics 2004, 60(1), 329-334.

Dawson LA, Mah K, Franssen E and Morton G, Target position variability throughout prostate radiotherapy. International Journal of Radiation Oncology, Biology, Physics 1998, 42(5), 1155-1161.

de Boer HCJ, van Sornsen de Koste JR, Creutzberg CL, Visser AG, Levendag PC and Hijmen BJM, Electronic portal image assisted reduction of systematic set-up errors in head and neck irradiation. Radiotherapy and Oncology 2001, 61, 299-308.

Denham JW, Dally MJ, Hunter K, Wheat K, Fahey PP and Hamilton CS, Objective decision making following a portal film; The results of a pilot study. International Journal of Radiation Oncology, Biology, Physics 1993, 26(5), 869-876.

Dobbs J, Barrett A and Ash D, Practical Radiotherapy Planning 3rd Edition, 1999, Arnold Publishers, London.

D'Souza WD, Lee S, DiBiase S, Amin P, Yu C and Regine W, Quantifying systematic and random setup uncertainties using daily ultrasound-based localization during prostate radiotherapy. International Journal of Radiation Oncology, Biology, Physics 2003, 57(2), Supplement.

el-Gayed AA, Bel A, Vijlbrief R, Bartelink H, Lebesque JV, Time trend of patient setup deviations during pelvic irradiation using electronic portal imaging. Radiotherapy and Oncology 1993, 26:162-171.

Fiorino C, Reni M, Bolognesi A, Cattaneo GM and Calandrino R, Intra- and inter-observer variability in contouring prostate and seminal vesicles: implications for conformal treatment planning. Radiotherapy and Oncology 1998, 47, 285-292.

Graham J, Gee A, Hilton S, McKenzie A, Hall C, and Appleby H, Geometric uncertainties in radiotherapy of the prostate and bladder, in Geometric Uncertainties in Radiotherapy: Defining the Planning Target Volume. The British Institute of Radiology, 2003.

Greener T, Practical determination of systematic and random set-up errors $\Sigma_{set\text{-}up}$ and $\sigma_{set\text{-}up}$ using portal imaging, in Geometric Uncertainties in Radiotherapy: Defining the Planning Target Volume. The British Institute of Radiology, 2003.

Greer PB, Mortensen TM, and Jose CC, Comparison of two methods for anterior-posterior isocenter localization in pelvic radiotherapy using electronic portal imaging. International Journal of Radiation Oncology, Biology, Physics 1998, 41(5), 1193-1199.

Hamilton, C.S. and Ebert, M.A. (2005) Volumetric uncertainty in radiotherapy, *Clinical Oncology*, **17**, 456-464.

Harms, W.B., Bosch, W.R. and Purdy, J.A. (1997) An Interim Digital Data Exchange Standard for Multi-Institutional 3D Conformal Radiation Therapy Trials. Leavitt, D.D. and Starkschall, G (eds). XII ICCR, Salt Lake City, Utah, May 27-30, 1997, Medical Physics Publishing, Madison, WI, pp. 465-468.

Hurkmans CW, Remeijer P, Lebesque JV and Mijnheer BJ, Set-up verification using portal imaging; review of current clinical practice. Radiotherapy and Oncology 2001, 58, 105-120.

ICRU Report 50. Prescribing, Recording, and Reporting Photon Beam Therapy. International Commission on Radiation Units and Measurement, Bethdesa, MD, 1993.

ICRU Report 62. Prescribing, Recording, and Reporting Photon Beam Therapy (Supplement to ICRU Report 50). International Commission on Radiation Units and Measurement, Bethdesa, MD, 1999.

Leaver D and Washington CM, Principles and Practice of Radiation Therapy 2nd Edition, Mosby, St Louis, 2004.

Little DJ, Dong L, Levy LB, Chandra A and Kuban DA, Use of portal images and BAT ultrasonography to measure setup error and organ motion for prostate IMRT: Implications for treatment margins. International Journal of Radiation Oncology, Biology, Physics 2003, 56(5), 1218-1224.

Litzenberg D, Dawson LA, Sandler H, Sanda MG, McShan DL, Ten Haken RK, Lam KL, Brock KK and Balter JM, Daily prostate targeting using implanted radiopaque markers. International Journal of Radiation Oncology, Biology, Physics 2002, 52(3), 699-703.

Livesy JE, Wylie JP, Swindell R, Khoo VS, Cowan RA and Logue JP, Do differences in target volume definition in prostate cancer lead to clinically relevant differences in normal tissue toxicity? International Journal of Radiation Oncology, Biology, Physics 2004, 60(4), 1076-1081.

Logue JP, Sharrock CL, Cowan RA, Read G, Marrs J and Mott D, Clinical variability of target volume description in conformal radiotherapy planning. International Journal of Radiation Oncology, Biology, Physics 1998, 41(4), 929-931.

Marieb EN and Mallatt J, Human Anatomy 3rd Edition, 2001, Addison Wesley Longman Inc.

McKenzie AL, van Herk M and Mijnheer B, The width of margins in radiotherapy treatment plans. Physics in Medicine and Biology 2000, 45, 3331-3342.

McKenzie AL, Coffey M, Greener T, Hall C, van Herk M, Mijnheer B and Harrison A, Technical overview of geometric uncertainties in radiotherapy, in Geometric Uncertainties in Radiotherapy: Defining the Planning Target Volume. The British Institute of Radiology, 2003.

Mutic S, Palta JR, Butker EK, Das IJ, Huq MS, Loo LND, Salter BJ, McCollough CH and Van Dyk J, Quality assurance for computer-tomography simulators and the computed-tomography-simulation process: Report of the AAPM radiation therapy committee task group No. 66. Medical Physics 2003, 30(10), 2762-2782.

Rasch C, Barillot I, Remeijer P, Touw A, van Herk M and Lebesque JV, Definition of the prostate in CT and MRI: A multi-observer study. International Journal of Radiation Oncology, Biology, Physics 1999, 43(1), 57-66.

Roach III M, Faillace-Akazawa P, Malfatti C, Holland J and Hricak H, Prostate volumes defined by magnetic resonance imaging and computerized tomographic scans for three-dimensional conformal radiotherapy. International Journal of Radiation Oncology, Biology, Physics 1996, 35(5), 1011-1018.

Roeske JC, Forman JD, Mesina CF, He T, Pelizzari CA, Fontenla E, Vijayakumar S and Chen GTY, Evaluation of changes in the size and location of the prostate, seminal vesicles, bladder, and rectum during a course of external beam radiation therapy. International Journal of Radiation Oncology, Biology, Physics 1995, 33(5), 1321-1329.

Rudat V, Schraube P, Oetzel Z, Zierhut D, Flentje M and Wannenmacher M, Combined error of patient positioning variability and prostate motion uncertainty in 3D conformal radiotherapy of localized prostate cancer. International Journal of Radiation Oncology, Biology, Physics 1996, 35(5), 1027-1034.

Seddon B, Bidmead M, Wilson J, Khoo V and Dearnaley D, Target volume definition in conformal radiotherapy for prostate cancer: quality assurance in the MRC RT-01 trial. Radiotherapy and Oncology 2000, 56, 73-83.

Smith, DP and Armstrong, BK, Prostate-specific antigen testing in Australia and association with prostate cancer incidence in New South Wales. The Medical Journal of Australia, 1998, 169: 17-20.

Stroom JB, Koper PCM, Korevaaar GA, van Os M, Janssen M, de Boer HCJ, Levendag PC and Heijmen BJM, Internal organ motion in prostate cancers patients treated in prone and supine treatment position. Radiotherapy and Oncology 1999, 51, 237-248.

Tortora G and Grabowski SR, Principles of Anatomy and Physiology 7th Edition, 1993, Harper Collins College Publishers.

Tinger A, Michalski JM, Cheng A, Low DA, Zhu R, Bosch WR, Purdy JA and Perez CA, A critical evaluation of the planning target volume for 3-D conformal radiotherapy of prostate cancer. International Journal of Radiation Oncology, Biology, Physics 1998, 42(1), 213-221.

van Herk M, Errors and margins in radiotherapy. Seminars in Radiation Oncology 2004, 14(1), 52-64.

van Herk M, Bruce A, Guus Kroes AP, Shouman T, Touw A and Lebesque JV, Quantification of organ motion during conformal radiotherapy of the prostate by three dimensional image registration. International Journal of Radiation Oncology, Biology, Physics 1995, 33(5), 1311-1320.

van Herk M, Remeijer P, Rasch C, and Lebesque JV, The probability of correct target dosage: dose-population histograms for deriving treatment margins in radiotherapy. International Journal of Radiation Oncology, Biology, Physics 2000, 47(4), 1121-1135.

Zelefsky MJ, Leibel SA, Gaudin PB, Kutcher GJ, Fleshner NE, Venkatramen ES, Reuter VE, Fair WF, Ling CC and Fuks Z, Dose escalation with three-dimensional conformal radiation therapy affects the outcome in prostate cancer. International Journal of Radiation Oncology, Biology, Physics 1998, 41(3), 491-500.